

AD-A036 319

HYDROSPACE RESEARCH CORP ROCKVILLE MD
INVESTIGATION OF HYDRODYNAMIC LOADING ON FAIRED TOWLINE, (U)
JUN 64 A BRISBANE, L I DAVIS, J J NELLIGAN NOBSR-91273
HRC-119

F/G 9/1

UNCLASSIFIED

NL

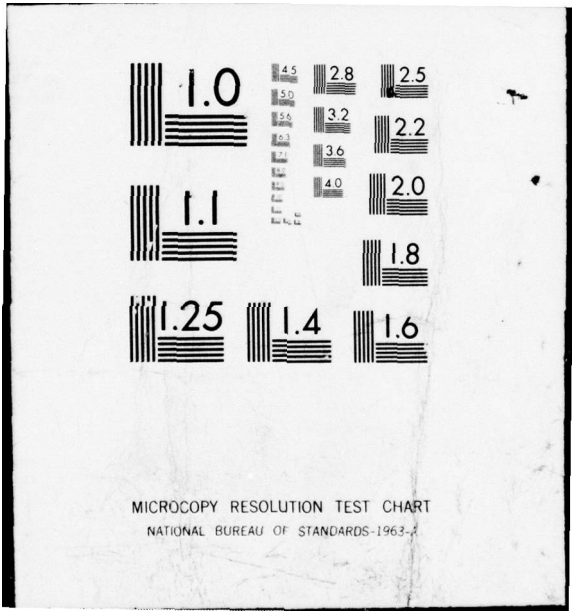
| OF |

AD
A036 319



END

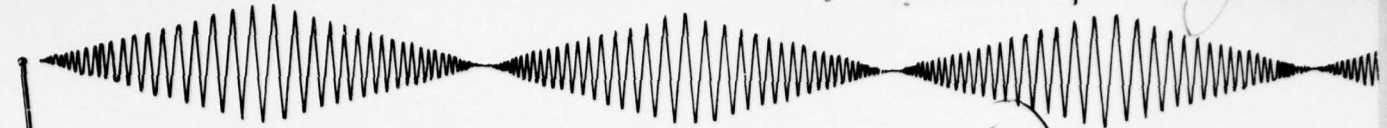
DATE
FILMED
3 - 77



MICROCOPY RESOLUTION TEST CHART
NATIONAL BUREAU OF STANDARDS-1963-A

ADA 036319

454 to



D D C
RECEIVED
MAR 3 1977
RESEARCH
A

HYDROSPACE RESEARCH CORPORATION



1749 ROCKVILLE PIKE
ROCKVILLE, MARYLAND

UNCLASSIFIED

~~CONFIDENTIAL~~

sp. 7

UNCLASSIFIED

HYDROSPACE RESEARCH CORPORATION
1749 Rockville Pike, Rockville, Maryland

This material contains information affecting the national defense of the United States within the meaning of the espionage laws, Title 18, U.S.C., Sections 793 and 794, the transmission or revelation of which in any manner to an unauthorized person is prohibited by law.

(1)

6 INVESTIGATION OF HYDRODYNAMIC
LOADING ON FAIRED TOWLINE

by

S. M. Gay, Principal Investigator

10 A./Brisbane,
L.I./Davis
J.J./Nelligan

12 69p.

DISTRIBUTION STATEMENT A
Approved for public release;
Distribution Unlimited

D.D.C.
RECORDS
MAR 8 1977
REG. 97

15 This work was performed under U. S. Navy Bureau of Ships Contract No. N0bsr-91273, Project Serial No. SF001 03 09, Task 8095.

11 17 June 1964

16 F00103
17 SF0010309

GROUP-4
Downgraded at 3 year intervals;
declassified after 12 years

14 HRC-119

January 15, 1965

Report No. 119

UNCLASSIFIED

174 550

CONFIDENTIAL

UNCLASSIFIED

21 January 1965

DOCUMENT RECEIPT

I hereby acknowledge receipt of the following:

**1 copy HRC Report No. 119, "Investigation
of Hydrodynamic Loading on Faired
Towline", dated 15 January 1965.**

Received by (signature)

DS.
Date received

UNCLASSIFIED

TABLE OF CONTENTS

	<u>Page</u>
<u>INTRODUCTION</u>	1
<u>BASIC CONSIDERATIONS</u>	3
<u>REVIEW OF THE DEVELOPMENT OF LOADING FUNCTIONS</u>	11
<u>TEST PROGRAM</u>	21
<u>TEST THEORY AND DESIGN</u>	21
<u>TEST EQUIPMENT AND FACILITY</u>	24
<u>TEST PROCEDURE</u>	39
<u>TEST RESULTS AND DISCUSSION</u>	41
<u>CONCLUSIONS AND RECOMMENDATIONS</u>	54
<u>REFERENCES</u>	55
<u>APPENDIX A</u>	56

INTRODUCTION

The faired towcable appears to be the key hydromechanical component of Variable Depth Sonar (V. D. S.) Systems. It is this component that serves to transmit propulsive forces and surface generated disturbances to the housing, transmits electrical power to the transducer and the electrical analog of the acoustic information back to the surface, resists attainment of depth, establishes maximum system forces, and complicates handling and storage. A clear understanding of the hydromechanics of towcables is thus a prerequisite to the satisfactory resolution of the many problems involved in sonar-system design.

One of the more important and timely aspects of this topic is the true nature of the hydrodynamic loads imposed on the towline by the flow. The magnitude and direction of this force determines the local rate of change of its inclination and tensile load. The hydrodynamic load is in turn affected by the shape, size, and inclination of the cable. A description of the variation of the hydrodynamic loads acting on a length of faired cable is called a "cable loading function", or simply, "loading function". It is evident that the prediction of towline characteristics, i. e., the forces, the depth and horizontal distance spanned, and the inclination, depends on the accuracy with which the force variation is described by the loading function.

Loading functions in current use are based on a combination of theoretical conjecture and limited experimental data. They are

CONFIDENTIAL

essentially two-dimensional in nature; a postulate fundamental to their derivation being that the flow about any section is identical with that existing on a rigid cylinder having the same shape and cross section. The results obtained on application of the various forms do not agree, and discrepancies between predicted and measured performance have been observed in the field.

This lack of basic agreement is of little consequence so long as cable lengths and towing speeds remain moderate. The discrepancies are, in fact, not obvious in either theory or practice under these conditions. However, the need for higher speeds and greater depths has forced recognition of the inadequacy of prediction based on existing methods. Moreover the suspicion has grown that the forces cannot be given the simple two-dimensional representation mentioned above.

Hydrospace Research Corporation was accordingly authorized to investigate the adequacy of existing loading functions and to effect an experimental determination of the loads on a real faired cable configuration, with the object of determining the agreement between that configuration and one based on the two-dimensional prediction techniques. This report contains an account of the work accomplished to date.

BASIC CONSIDERATIONS

We restrict our considerations to steady-state (no time dependence), plane configurations. The plane is that one defined by the direction of gravity and the direction of translation of the towing vessel. The towed system is thus considered to translate rectilinearly in the direction normal to gravity. Configurations not lying wholly within this plane are of practical interest. Such configurations are said to "kite". Kiting, however, is an undesirable phenomenon and the interest in this area, from the VDS standpoint, is in a sufficient understanding of the effect on system geometry to correct the cause rather than to predict the degree.

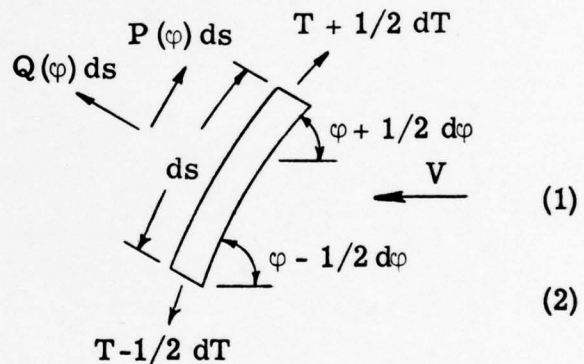
The scope of this problem is thus reduced to consideration of an idealized towing configuration. Such configurations are, however, of great practical significance in the design of VDS systems.

It is necessary to compute or predict the towing configuration in both the design and operation of a VDS system. Specifically, under steady tow, for a given speed of advance and scope of towline it is desired to predict the depth, trail, and the average towcable tension. These are required to intelligently locate the sonar beneath the thermocline, or advantageously with respect to the towing vessel to optimize detection capabilities. Knowledge of the sonar position with respect to the vessel is an aid in fire control. Prediction of towline tension is fundamental in design of the system from an operational and safety standpoint.

Computation of the equilibrium configuration of a cable-towed system in terms of its geometry and towline tension involves consideration of both the towline and the towed body. The individual forces acting on these components must be determined and the way in which they combine to produce the configuration must be defined. Gravitational, displacement, and hydrodynamic forces are involved.

In treating the problem of computing the configuration, the body and towline are separable.

Examining the towline first, the equations describing the equilibrium of an incremental segment of flexible towline may be written, as by Pode^{1*} and others:



$$dT = -P(\varphi) ds.$$

and

$$Td\varphi = -Q(\varphi) ds.$$

where T is the internal tensile force, φ the angle of inclination of the element of fairing relative to the direction of motion, and P and Q , external forces per unit length, as illustrated on the sketch. V is the velocity of tow and s , the cable-length coordinate.

Eliminating ds and integrating:

$$\frac{T}{T_0} = \exp \left(\int_{\varphi_0}^{\varphi} \frac{P(\varphi)}{Q(\varphi)} d\varphi \right) \tag{3}$$

*References are listed on Page 55.

where T_0 and φ_0 represent known values of tension and angle at some reference point, P_0 , along the cable. Substituting (3) into (2) and integrating gives

$$s = \int_{\varphi_0}^{\varphi} \frac{T_0}{-Q(\varphi)} \exp \left(\int_{\varphi_0}^{\varphi} \frac{P(\varphi)}{Q(\varphi)} d\varphi \right) d\varphi \quad (4)$$

the distance along the towline from P_0 to P . Employing the geometric relations $dx = \cos \varphi ds$ and $dy = \sin \varphi ds$, the vertical distance (depth) and horizontal distance (trail) may similarly be expressed:

$$y = \int_{\varphi_0}^{\varphi} \frac{T_0}{-Q(\varphi)} \exp \left(\int_{\varphi_0}^{\varphi} \frac{P(\varphi)}{Q(\varphi)} d\varphi \right) \sin \varphi d\varphi, \quad (5)$$

and

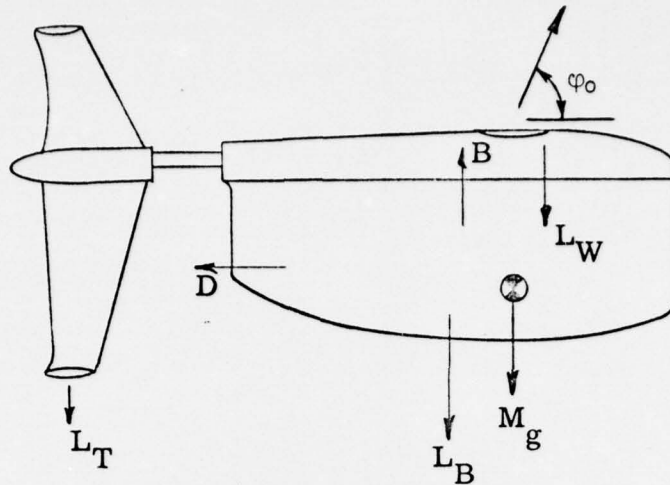
$$x = \int_{\varphi_0}^{\varphi} \frac{T_0}{-Q(\varphi)} \exp \left(\int_{\varphi_0}^{\varphi} \frac{P(\varphi)}{Q(\varphi)} d\varphi \right) \cos \varphi d\varphi. \quad (6)$$

Thus the configuration may be determined in terms of tension, scope, body depth, and trail for a given set of end conditions T_0, φ_0 if the functions $P(\varphi)$ and $Q(\varphi)$ are known.

Departing from the towline for a moment, consider the requirement for specification of the boundary condition in the solution of the problem. The boundary condition (T_0, φ_0) represents the force developed by the sonar housing (refer to the following sketch). The force includes the individual components resulting from:

1. weight, Mg ,
2. buoyancy, B ,
3. hydrodynamic drag, D ,
4. hydrodynamic lift, L_W, L_T, L_B ,

where M is the mass of the housing, g the acceleration of gravity, and the subscripts W, T , and B refer to the wing, tail, and body respectively.



The forces are resolved in the normal way:

$$T_o = \sqrt{Mg - B + L_B + L_W + L_T^2 + D^2}$$

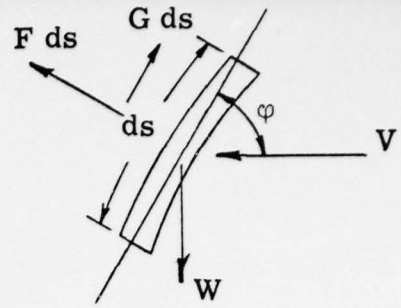
and the angle at which the resultant force acts is:

$$\phi_o = \tan^{-1} \left(\frac{Mg - B + L_B + L_W + L_T}{D} \right)$$

The balance of moments establishes the trim (pitch angle) of the body for a particular towpoint location. For equilibrium then, the tension and angle of the towline at the body must be such as to counterbalance the forces developed by the body.

T_o and ϕ_o represent the end conditions as developed by the body, and establish the reference point from which the integration of the towline configuration equations may commence.

With the boundary condition specified, we return to the solution of Equations (3) through (6). Obviously the terms $P(\phi)$ and $Q(\phi)$ must be specified. These terms represent the incremental external force components resolved in directions normal and tangential to the element. The forces acting are static -- weight, buoyancy, and hydrodynamic forces.



Letting W represent the weight per unit length of the element in water, the static force components normal and tangential to the element are respectively $W \cos \varphi$ and $W \sin \varphi$.

Letting F and G represent normal and tangential components of the hydrodynamic force acting on the elements, the loading functions may be written in the following manner:

$$Q(\varphi) = F - W \cos \varphi, \quad (7)$$

and

$$P(\varphi) = G - W \sin \varphi. \quad (8)$$

The solution to the problem now depends on specification of the hydrodynamic loading functions, F and G . From what is known of the nature of hydrodynamic forces a list of probable influencing parameters can be formed:

1. velocity of tow
2. fairing type, thickness, chord length, surface roughness
3. fluid density and viscosity
4. angle of inclination to the flow.

These represent a minimum listing of the important parameters.

The influence of other factors is suspected, e. g., the effect of the flow over neighboring elements on the hydrodynamic force on a particular element.

Forms for the loading functions, recognizing some or all of the listed parameters, have been postulated by previous investigators. Methods for computing the configuration based on these functions have

been available for some time. However, the agreement between methods is poor. Furthermore, the little data available from full scale tests do not substantiate any of the methods in present use.

Returning now to Equations (7) and (8), we observe that if F and G are functions only of the angle and speed, we may write

$$F = F(\pi/2) F'(\varphi) \quad (9)$$

and

$$G = G(0) G'(\varphi), \quad (10)$$

where $F'(\varphi)$ and $G'(\varphi)$ are functions of the angle only. Now $F(\pi/2)$ is the resistance per unit length of the towcable when normal to the stream. It is, then, just the drag per unit length. In cable work, this value is typically designated by the symbol "R". The similarity principle mentioned earlier permits the measure of R to be taken from a strut of similar cross-sectional shape. Similarly, $G(0)$ is the tangential force per unit length when the cable is parallel to the stream. ●

In general, the values of R and $G(0)$ depend on the velocity of tow and the shape and size of the fairing. We may define force coefficients, C_R and C_G , as follows:

$$C_R = R / \frac{1}{2} \rho V^2 d$$

and

$$C_G = G(0) / \frac{1}{2} \rho V^2 d,$$

where ρ is the mass density of the fluid (e. g., sea water) and d is a typical measure of length taken on the right-section of the fairing. The breadth, or frontal width, is usually selected for this measure.

C_R and C_G are not necessarily constant. Values of C_R

measured at identical values of the ratio Vd/ν , where ν is the kinematic viscosity, are constant, however, whereas values of C_G measured at identical values of that parameter are not necessarily constant.

The ratio described above is a measure of the ratio of shearing (viscous) forces to the kinematic forces. It is thus a measure of the relative retardation of the fluid in its passage over an object and is hence a measure of the momentum transferred to the fluid, or conversely, the viscous drag forces acting on the body. The proper length for computation of this ratio is evidently the length over which a particle of fluid is in contact with the body.

An essential difficulty with application of the concept of $G(0)$ is immediately evident. Its value depends on the length of cable parallel to the flow. Since this cannot be established a priori for any given configuration, the value of the measure of $G(0)$ is doubtful.

An artifice commonly used to generalize the results of Equations (4), (5), and (6) is to define the non-dimensional ratios σ' , η' , and ξ' as follows:

$$\sigma' = \frac{Rs}{T_0} = \int_{\varphi_0}^{\varphi} \left[\frac{\exp\left(\int_{\varphi_0}^{\varphi} \frac{P(\varphi)}{Q(\varphi)} d\varphi\right)}{\frac{-Q(\varphi)}{R}} \right] ,$$

$$\eta' = \frac{Ry}{T_0}, \text{ and } \xi' = \frac{Rx}{T_0} .$$

$Q(\varphi)/R$ then takes the form $F'(\varphi) - \frac{W}{R} \cos \varphi$. Hence, if $F(\varphi)$ can be expressed in the form of Equation (9), the first term of the expression for $Q(\varphi)/R$ becomes a function of φ alone.

The value of φ that satisfies the identity $Q(\varphi)/R = 0$ is known as the critical angle. The curvature, from Equation (2), is identically zero in this case, and the cable configuration is accordingly an uncurved (straight) line.

REVIEW OF THE DEVELOPMENT OF LOADING FUNCTIONS

As mentioned earlier, a number of forms have been proposed for the cable loading functions. We shall review these briefly in this section.

Historically, the solution to the problem of predicting the shape of a cable loaded by its own weight has been known for several centuries. The first known work on the shape of cables under hydrodynamic loads evidently occurred early in the 20th century in an effort to meet normal and aerodynamic requirements, and to solve some of the mechanical problems in the transmission of electrical energy via above ground conductors.

Relf and Powell² evidently performed the first consistent experiments to determine the effect of oblique flows on the hydrodynamic loading of round cables. The classic result, $F/R = \sin^2 \varphi$, was obtained. This result formed the basis for Glauert's³ computation of the shape assumed by the cable. This work culminated in the generalized solutions presented by Pode in 1951.

We note that the earlier experimental work did not encompass the measure of the tangential loads, G . Pode required this factor to proceed with his work, however, and analyzed a considerable volume of test data taken with straight cables for this purpose at DTMB in the late forties. His results exhibited considerable scatter, and he concluded that the most reasonable conclusion warranted was that the tangential force was independent of the cable's aspect to the flow.

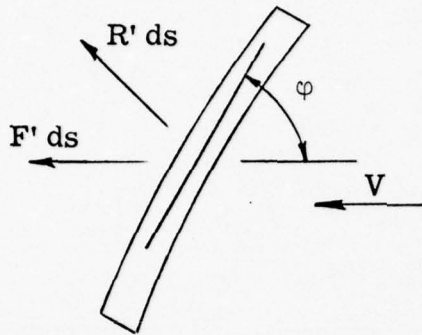
Since this form for the tangential component also resulted in considerable mathematical simplification, it was adopted for the work mentioned above.

These results sufficed for the earlier applications (towed pitot heads for aerial use and paravanes, kites, and depressors for naval use) which utilized moderate lengths of essentially round cable. The high resistance and unsteady forces on round cables soon led to efforts to effect reductions in the normal resistance, R , and the discovery that the fairly simple law for round cables was not applicable.

Inasmuch as no particular merit occurred to any given representation of the loads, Pode extended his work to encompass the higher values of G that must attend the increased wetted area of faired cable, but retained the basic assumption of aspect-independence discussed above. Since the tangential load is assumed to be constant, it appears as a parameter $f = G/R$ in Pode's work. The value of f is taken to be in the range 0.01 to 0.03 for round cable, and a single value, 0.1, is given for faired cable. The $R \sin^2 \varphi$ law was assumed to hold for the normal component of the force. These results were not based on any additional experimental work.

Other approaches to the prediction of loads on faired cables generally proceed on the assumption that the frictional and pressure components of the hydrodynamic load can be treated separately. This approach was suggested by Reber⁴ as an outgrowth of computation of the effect of a linear distribution of streamline floats on the configuration of a heavy, round cable towed in a horizontal plane. The function of the

floats was to support the weight of the cable, and though distributed discretely, were treated mathematically as though uniformly distributed, as indicated on the inset sketch. The loading functions are



then

$$F = R' + F' \sin \varphi \text{ and}$$

$$G = -F' \cos \varphi.$$

The concept is plausible in that the resultant of the pressures must be a force acting normal to the surface.

This component is assumed to vary as $\sin^2 \varphi$ as on a bare round cable. The frictional component is concurrent with the flow lines which are taken as concurrent with the remote velocity. In essence, the local flow is assumed to be undisturbed by the pressure gradient along the fairing, hence two-dimensional.

Podé effected solutions for these functions for neutrally buoyant cables. Eames⁵ also treated this concept, in a more general fashion, and effected solutions for certain special cases, including the case of a very thin (high fineness ratio) fairing for which the pressure drag is negligible. In this case F' is a function of the flat-plate area only and hence is independent of the aspect, if the slight changes in the frictional force coefficient due to the changing path length of the flow is neglected.

Whicker⁶ also made use of the separability of the pressure and

frictional forces to arrive at forms for the normal and tangential force coefficients:

$$C_n = C_R \left(a + \frac{V}{V_n} b \right)$$

and

$$C_t = C_R \left(d + \frac{V}{V_t} e \right),$$

where C_R is the force coefficient of the faired section when perpendicular to free stream velocity, V , a and d are components of the force coefficients due to pressure forces, and $\frac{V}{V_n} b$ and $\frac{V}{V_t} e$ are components due to the friction force.

Writing the basic force equation as

$$F = C_n \rho / 2 \cdot K \cdot V_n^2$$

and

$$G = -C_t \rho / 2 \cdot K \cdot V_t^2,$$

where K is a reference dimension, one finds on substitution for C_n and C_t ,

$$F = C_R \rho / 2 K \left[a V_n^2 + b V V_n \right] = R \left[a (V_n/V)^2 + b (V_n/V) \right]$$

$$G = -C_R \rho / 2 K \left[d V_t^2 + e V_t V \right] = -R \left[d (V_t/V)^2 + e (V_t/V) \right]$$

where $R = C_R \rho / 2 K V^2$.

Employing $V_n = V \sin \varphi$ and $V_t = V \cos \varphi$, these assume the form

$$F = R \left[a \sin^2 \varphi + b \sin \varphi \right]$$

$$G = -R \left[d \cos^2 \varphi + e \cos \varphi \right]$$

The data on circular cylinders taken by Relf and Powell and later data taken by Powell on a 4:1 fineness-ratio streamline strut were utilized to determine the coefficients a , b , d , and e . Then, assuming a linear relation between these coefficients and the ratio of the thickness

to chord (t/c), the values of the coefficients were determined as a function of t/c . The following result was obtained:

$$F/R = (1 - t/c) \sin \varphi + t/c \sin^2 \varphi$$

$$G/R = - (0.386 - 0.303 t/c) \cos \varphi - (0.055 - 0.020 t/c) \cos^2 \varphi .$$

Whicker recognized the danger of establishing the force coefficients on the basis of such limited data, and yet these were all that were then available.

Powell's data, converted to normal and tangential form and non-dimensionalized by dividing by R , are shown in Figures 1 and 2. It can be seen that the \sin^2 law would underpredict the normal force component in this case. In Figure 2 the G term is seen to reach a maximum value at about 30° , then diminish almost linearly with increasing φ . The discrepancy involved between using a constant G/R value of 0.1 suggested by Pode and using a G loading function based on Powell's data (as Whicker) is clear. In the region of most practical importance, between $\varphi = 20^\circ$ and $\varphi = 60^\circ$, Powell's G term is from 40% to 170% higher.

More recently the Admiralty Experiment Works at Haslar has performed similar tests on rigid strut section simulating fully enclosed continuous fairing⁸. The tests were performed in water in a towing basin. Three different lengths were tested and the differences were used in computing the forces, thus minimizing end effects.

These two sets of two-dimensional data (Powell and AEW) are consistent in at least two respects; the experimental curves of the normal force fall above the $\sin^2 \varphi$ curve while following its general trend, and the shapes of the two tangential force curves are similar to each other, showing

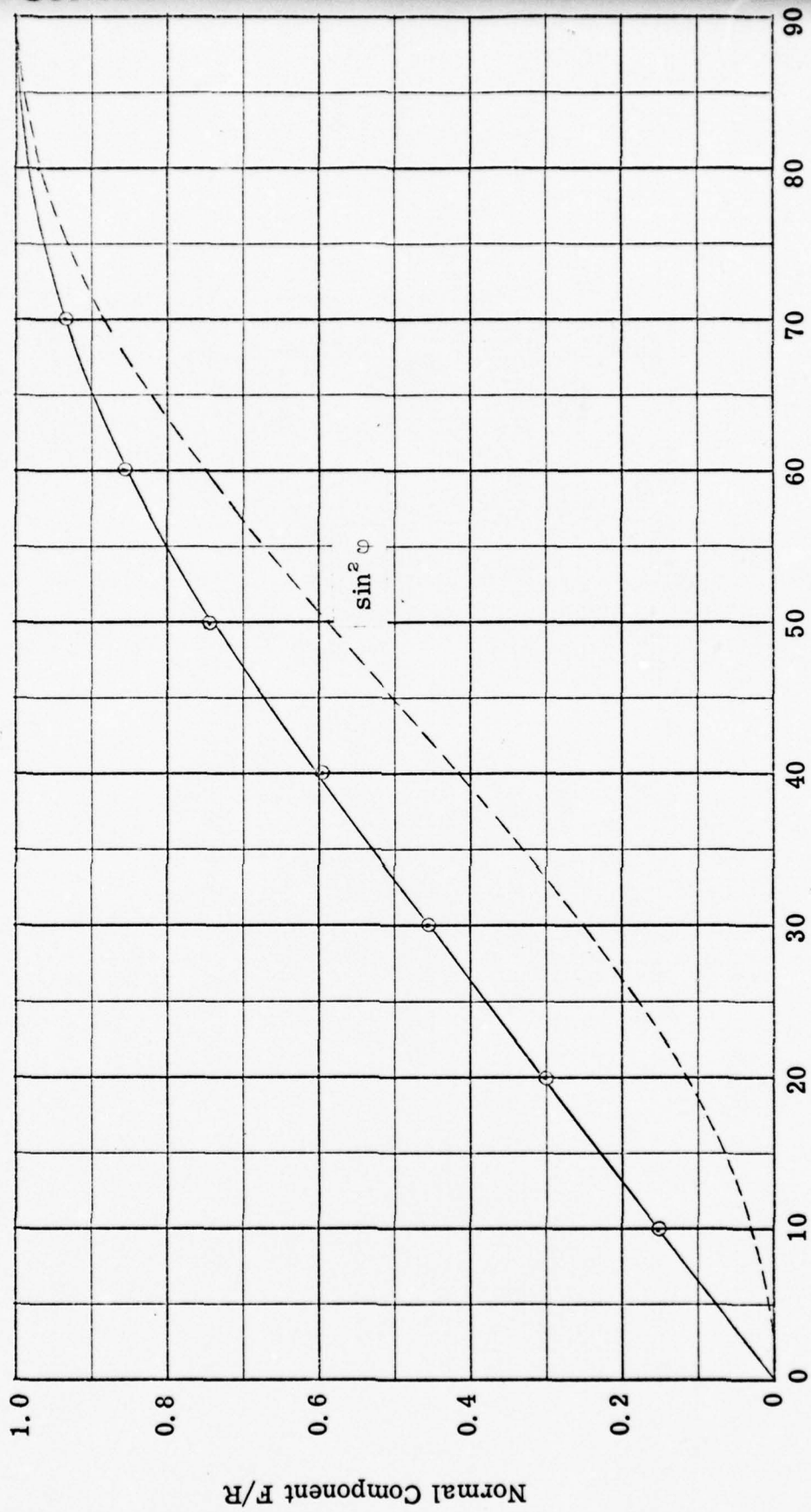


Figure 1 - Normal Component of Force on a Strut vs Angle of Inclination (Powell)

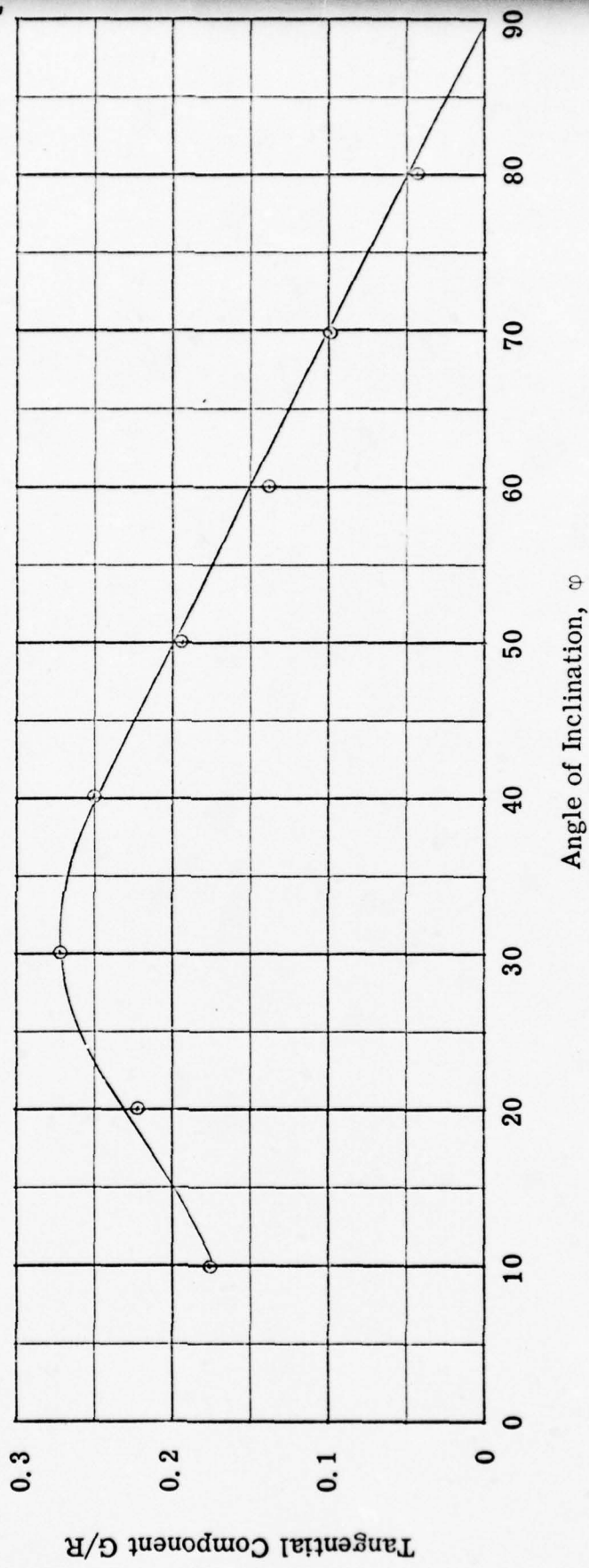


Figure 2 - Tangential Component of Force on a Strut vs Angle of Inclination (Powell)

maximum values in the $\varphi = 30^\circ$ to 40° range. The AEW data as published show a consistent spread with velocity, indicating a Reynolds number effect. Accounting for Reynolds number effect on R when non-dimensionalizing does not eliminate the spread.

On the basis of the AEW data, Lofft has suggested a quadratic relation between the force coefficients and the thickness-ratio. Numerical values based on the AEW results and Powell's data were published.

The above tests constitute the known, applicable, and available works. A second possible source of data was investigated; tests at sea on full scale systems. Reports by DRL and TRACOR on sea trials of VDS systems were reviewed. The information in these reports was considered not applicable in determining the steady-state loading functions for two primary reasons. First, the tests were not conducted with the object of obtaining the loading functions and therefore the systems were not properly instrumented. Second, the tests performed from a destroyer in normal sea conditions do not approach steady-state.

DTMB recently conducted tests at sea on a fully instrumented, faired cable/body system to obtain information on the loading functions. The report has not yet been published.

The Powell and AEW data represent the only experimental basis for presently used loading functions. As a result, with unsubstantiated hypotheses the only alternative, these data have been pressed to apply to fairings to which they bear little resemblance. The question arises as to the validity of such extrapolations.

Powell's strut and the AEW strut were rigid, smooth models of particular cross-sectional shapes and fineness ratios. Fairings to which the data have been applied include trailing, clip-type and sectional of various shapes and fineness ratios.

Also, the data from the wind tunnel and water-channel on a rigid strut are essentially two-dimensional. The faired towline, in general, sees three-dimensional flow. Thus, it is questionable that the two-dimensional data are directly applicable to fairing as configured in a towline.

When examining the basis for the loading functions in present usage, it is not unexpected that correlation between configurations predicted by the various methods is not good. The cause for this was well recognized by those who proposed loading functions, i. e., the lack of experimental basis for the establishment of the functions.

In conclusion we shall mention a form suggested by Landweber, namely $F/R = \sin^2 \varphi$ and $G/R = -\cos^2 \varphi$. He observes, however, that experimental results are more closely satisfied by $G/R = -\cos \varphi$. This formulation is used by at least one corporation engaged in the design and production of VDS Systems.

Of the loading functions mentioned above, the ones ascribed to Pote, Eames, and Whicker are in most common use. It has been remarked that results obtained on application of these loading functions yield significantly different results. To illustrate, consider the answers obtained for the question, "what is the minimum force and cable size

required to tow a body of reasonably small drag at a specified depth and speed?"

Assuming a constant value of the maximum tensile stress in the cable, resistance coefficients and starting angle, φ_0 , between the systems, the following result is obtained for $\varphi_0 = \pi/2$ and zero critical angle:

$$T_E/T_P = 3.8,$$

$$T_W/T_P = 1.45, \text{ and}$$

$$T_E/T_W = 2.6; \text{ and}$$

$$d_E/d_P = 1.95,$$

$$d_W/d_P = 1.2, \text{ and}$$

$$d_E/d_W = 1.61.$$

Here T_E stands for tension computed according to Eames, T_P for tension computed according to Pode, etc., and d_E for fairing width computed according to the particular function derived by the author designated by the subscript.

The significance of the variation is believed to be self-evident.

TEST PROGRAM

On the basis of the foregoing, it was decided that the most direct approach to resolution of the loading-function problem was to obtain measures of the hydromechanical loads directly from a real configuration. As with all experimental work, certain practical considerations impose limitations on the experimental technique. These and the theory underlying the test, the equipment and procedures employed are presented in this section.

TEST THEORY AND DESIGN

The theory underlying the tests is simple and direct. Consider Equations (1), (2), (7) and (8). Substitution of (7) and (8) in (1) and (2) yield the following equations;

$$\frac{dT}{ds} = - (G - W \sin \varphi) \quad (1.1)$$

and

$$\frac{d\varphi}{ds} = - (F - W \cos \varphi). \quad (2.1)$$

These equations merely express the static force balance that must obtain on the assumption of a plane configuration containing the gravitational vector and negligible bending moments in the fairing and cable. As such, they are independent of any assumption regarding the nature of F and G.

If, then, values of tension and angle can be measured as a function of length on a faired section of known weight and at a known speed, all values necessary for the solution of (1.1) and (2.1) are available.

This is the basis for the experiment.

The ideal experiment would consist of obtaining simultaneous measures of the tension and angle at closely spaced intervals along a long cable towed at constant speed. This procedure would require depths obtainable only at sea and a very expensive specially designed and constructed test fairing.

An alternate approach consists of obtaining the desired measures at the surface and changing the scope for each run. This procedure is as valid as the one outlined above, provided that no element of the fairing is affected by the presence of the elements situated farther up the towline. But the latter is an effect we seek to discern.

The simplification resulting from adoption of this approach was overpowering, however, in view of the fact that the experiment itself was exploratory in nature and would require considerable work just to establish the proper techniques for its application. Moreover it can be demonstrated that an effect of the sort postulated above would be discernable by comparison of depths or rate of change of depth with scope, predicted on the basis of the measurements.

A question arises as to the accuracy required in the measures. An error analysis was conducted and it was determined that results of reasonable accuracy could be obtained with available instrumentation provided care were taken not to degrade inherent sensor accuracy in the signal processing and recording equipment.

Of even greater importance, it is absolutely necessary that the test fairing be steady and stable under tow and give repeatable results.

As will be discussed later, the fairing utilized for these tests left much to be desired in this report.

A selection of the desired conditions thought necessary to conduct a fruitful test program was made. Steady-state towing, or as close to steady-state conditions as possible was needed. The size and the incremental length of the cable and fairing used had to be large enough to produce measureable forces, yet small enough to facilitate practical handling techniques and equipment. Forces, on the other hand, had to be small enough to allow a good range of cable angles and towing speeds. Based on these considerations plus the error analysis, it was decided that the Hydrospace Research Corporation test facility in Martinsburg, West Virginia would give close to steady-state conditions, and would be suitable to conduct such a program. It was also decided that a 0.3-inch diameter cable and fairing, tested in 10 foot increments, would meet the remaining requirements.

In order to tow such a faired cable, a multi-purpose depressor was needed. This depressor had to meet the following requirements: be stable under steady tow; produce downward forces large enough to control the behavior of the tow line; produce constant T_0 and φ_0 at constant speed; and be large enough to house required bottom end instrumentation.

The instrumentation for the test program included that required to measure tension and towline angle at the surface and tension and angle at the body, body depth and attitude, and towing speed.

TEST EQUIPMENT AND FACILITY

The apparatus used to conduct the test program consisted of: a faired cable; a modified 1/4-scale model of the AN/SQA-8 providing the known end conditions for the towcable; a custom towing frame from which the test model was towed; and the instrumentation for measurements, including a specially designed speed measuring instrument.

Fairing and Cable

The fairing used was the fully enclosed continuous rubber fairing, DTMB No. 7 shape with a maximum thickness of 0.5 inch and a fineness ratio of 6. The fairing encloses a 0.3-inch diameter double-armor steel cable which contains 6 electrical conductors and has a breaking strength of 6,000 lbs. The towline weighed 0.2 lb/ft in water.

The fairing was installed on the cable in three separate sections of 25, 50, and 16 feet respectively. The fairing was supported approximately every 22 inches along its length by a brass and a steel ring inserted into a notch in the leading edge of the fairing. The brass ring was swaged on the cable with a modified Nicopress handtool, with the steel ring floating next to the brass ring to act as a thrust washer. The notches for the rings were then covered and the joints between the sections of fairing were spliced to make a smooth and continuous piece of fairing.

Body

The body used in the investigation was a modified 1/4-scale model of the AN/SQA-8 furnished to Hydrospace Research Corporation by

the David W. Taylor Model Basin. The body is 3.4 feet long, 0.833 feet across the beam, and 1.125 feet high. Fully instrumented and ballasted for test, it weighed 199 lbs in air and 151 lbs in water. The body was modified by relocating the towpoint in order to accommodate the instrumented towstaff. To maintain body stability in view of the new towpoint location, the tail boom was extended to its most rearward position.

The body housing contained two watertight containers, one of which housed pitch and roll pendulum pots, a pressure transducer to measure depth, and the associated electronics for the bridge-type transducer (see Figure 3). The second can contained the 26-volt battery pack which supplied the power to the electronics in the body. Body instrumentation not housed in a can included a pendulum pot attached to the towstaff to measure towstaff angle, and an "S"-type, strain gaged, flexure to measure towline tension at the body. Figure 4 is a photograph of the model AN/SQA-8.

Towing Frame

A custom towing frame was designed to:

1. provide a towpoint so that towline water entry occurred out of the wake of the towboat and in relatively undisturbed water,
2. provide a means of transmitting the towing load from the faired cable to the tension dynamometer without damaging the fairing in any way,
3. store the fairing, and

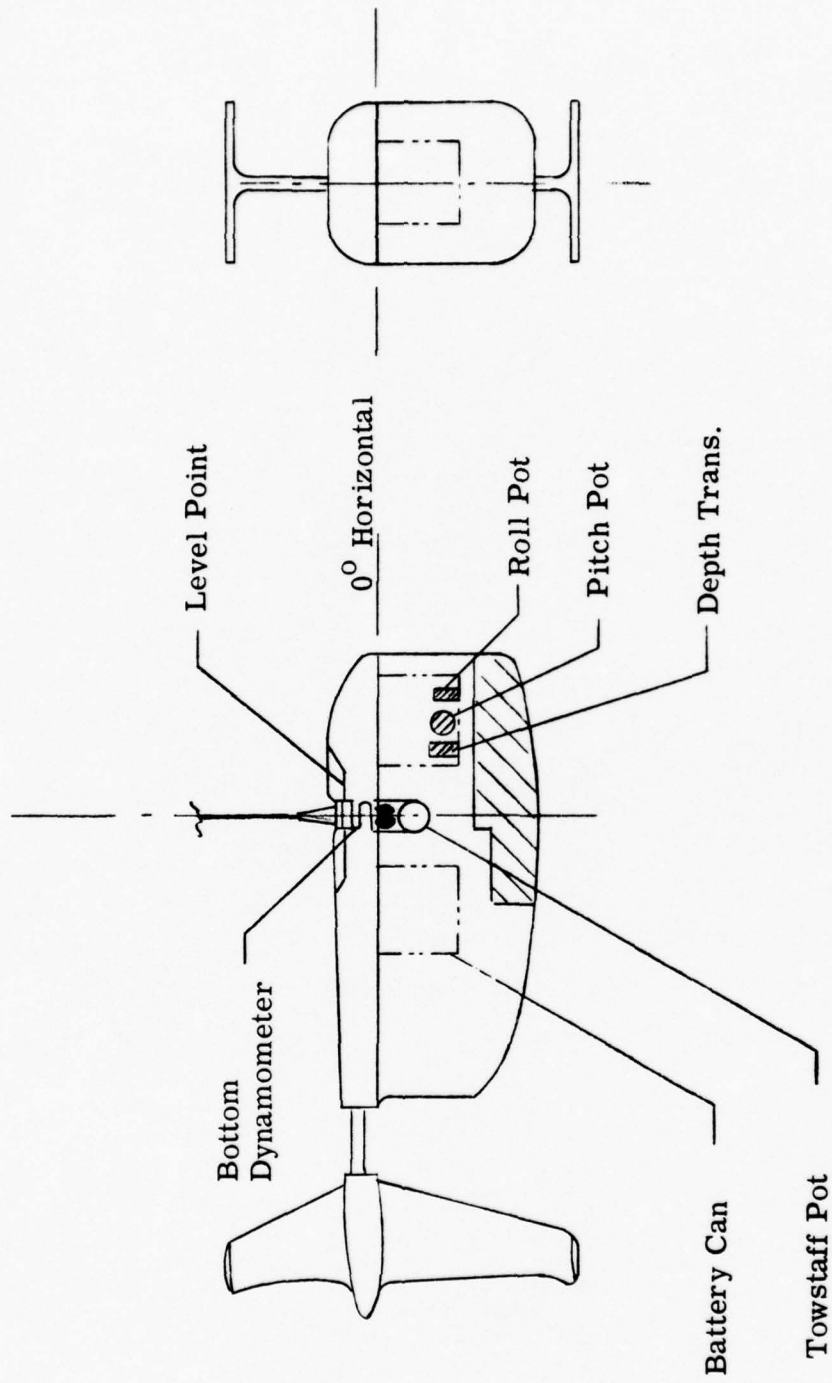


Figure 3 - Body Instrumentation

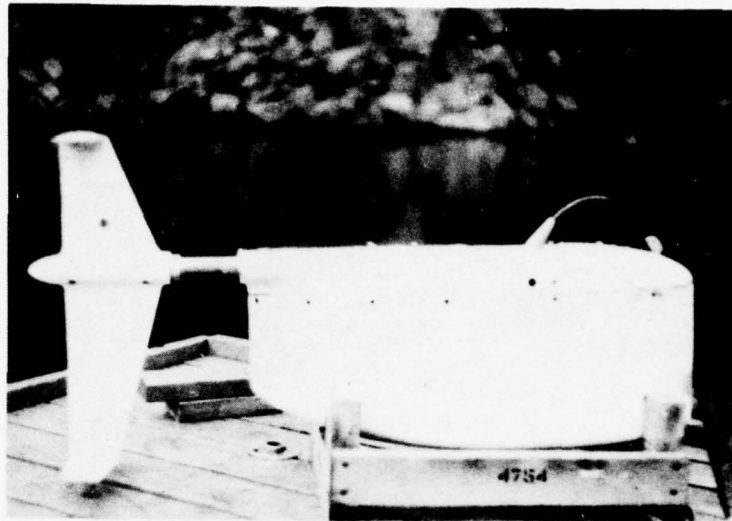


Figure 4 - Modified 1/4 Scale Model AN/SQA-8



Figure 5 - Towing Frame Configuration

4. provide a means for regulating scope in the water and the amount of fairing in the air.

The towing frame consisted of two 4-inch aluminum I beams 30 inches apart and 16 feet long. The towline storage drum was mounted in two adjustable bearing blocks bolted on the side plates suspended from the left end of the I beams. The suspension bracket for the 300-lb top tension dynamometer was located on the top side of the frame at the left end of the drum. The towing load was transmitted directly to the storage drum whose shaft floated in ball bearings. The drum was restrained from rotating under towing load by an arm clamped to the shaft and restrained at the other end by the dynamometer. The arm was twice as long as the drum radius so that a 2 to 1 advantage was realized. This allowed use of a smaller range dynamometer of higher accuracy, the accuracy of the transducer being a percent of its full-scale rating.

A swivel and shackle attached to the starboard side of the tow frame served as the towpoint for the towboat speed measuring device.

The towing frame was mounted just aft of midship with the drum extended over the port side in order that the fairing would be in the least disturbed water, as shown in Figure 5.

The top angle potentiometer was clamped on the fairing between the drum and water line in a position that would keep it out of the influence of the water and at the same time would not contact the drum at the shallow towing angles. The device is shown in Figure 6.

A fairing guide was designed for the correct alignment of the

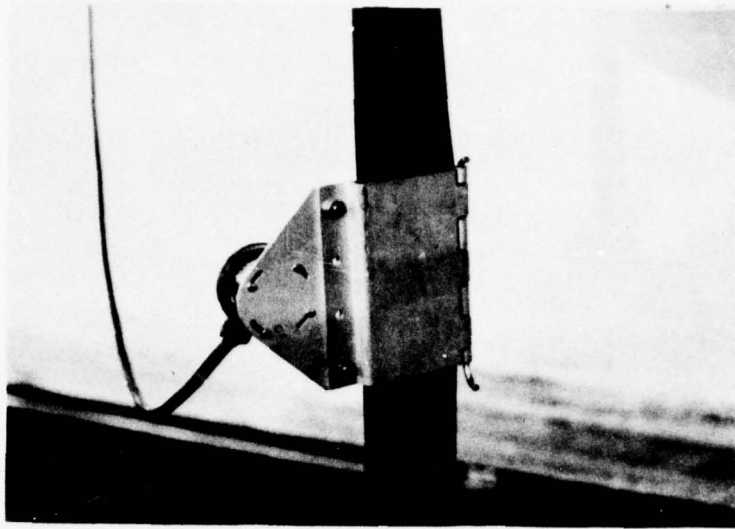


Figure 6 - Top Angle Measuring Device

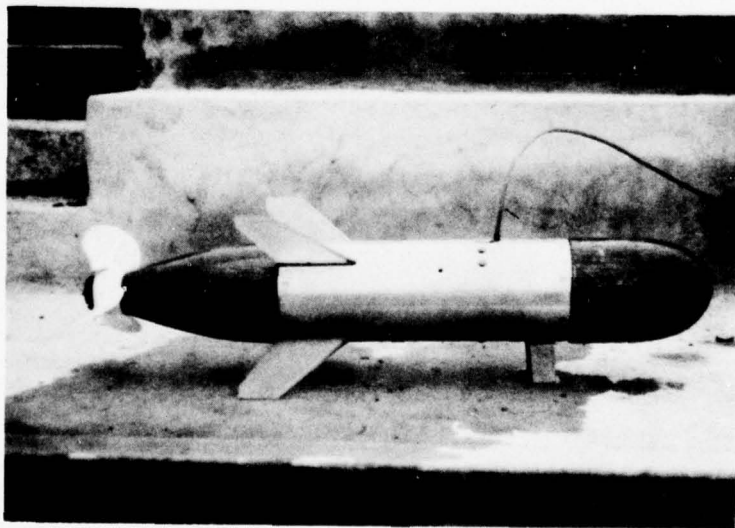


Figure 7 - Speed Measuring Instrument

fairing to assure the accuracy of the top angle potentiometer measurements.

Speed Measuring Instrument

This instrument was especially designed for this project because of the requirement to measure speed accurately and the fact that no other instrument was available.

The housing of the instrument is a body of revolution, 42 inches long, 6.6 inches in diameter, and weighing approximately 50 lbs in water. Figure 7 is a photograph of the device.

It was given a preliminary towing test at the Hydrospace Research Corporation towing facility at Martinsburg, West Virginia, to assure that it was hydrodynamically stable. The instrument proved stable over a speed range through 30 knots.

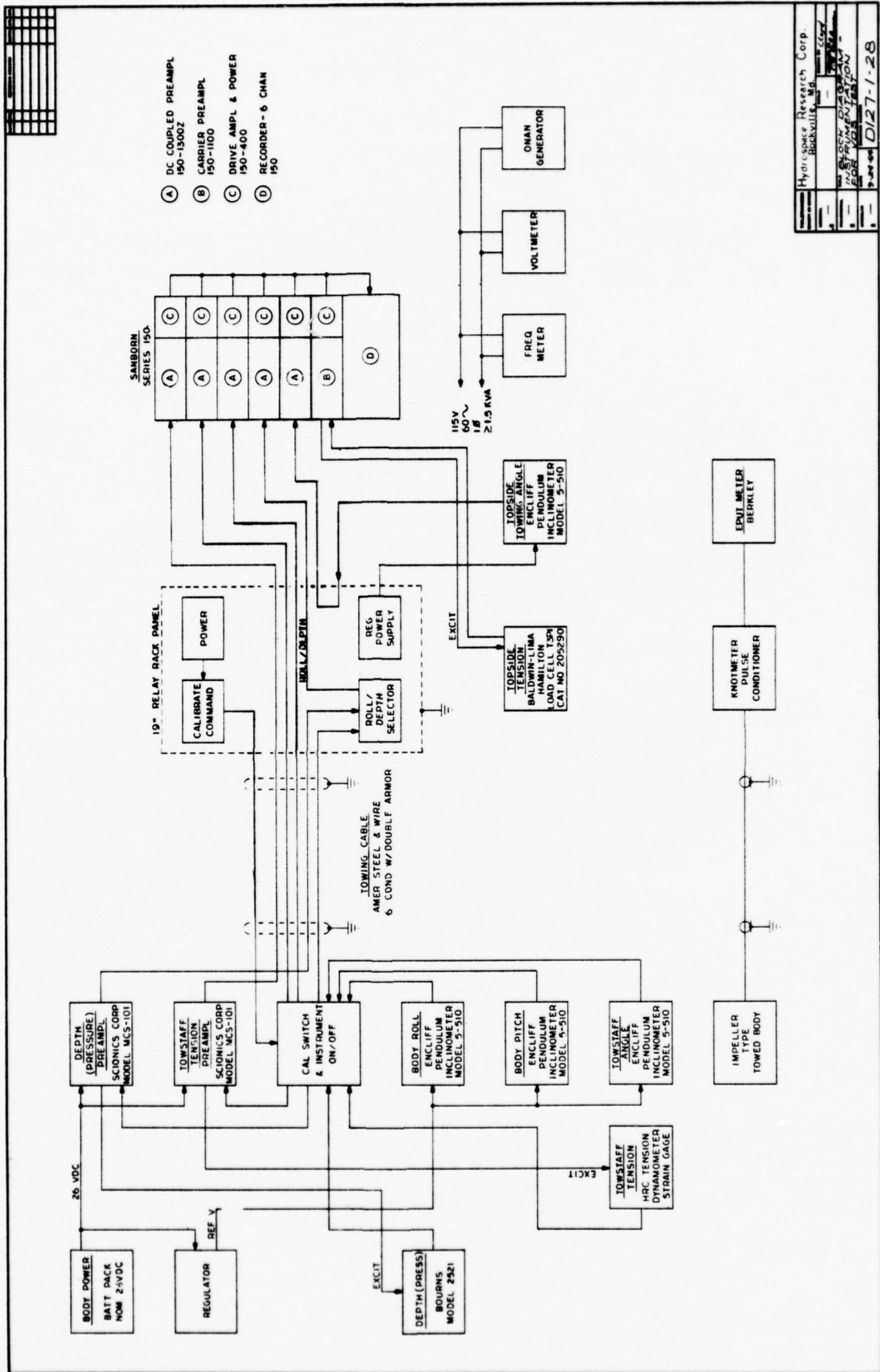
The speed measuring instrument was then calibrated at the University of Michigan towing tank, at Ann Arbor. The slope of this curve is given in the Instrumentation Section.

Instrumentation

Reference is made to Figure 8 which is a functional block diagram of the system of instrumentation provided for the acquisition of data during the towing tests.

As shown, eight transducers were provided to indicate the magnitude of towing speed, body depth, body roll, body pitch, towstaff tension and angle at the body, and towing tension and angle at the towboat.

Towing speed was measured by towing a body of revolution fitted with an impeller whose speed of rotation was directly proportional



Hydrospace Research Corp	
Baltimore, Md	
1/27/54	
INSTRUMENTATION	
FOR VOS TEST	
9-1-54	
DI27-1-28	

Figure 8 - Instrumentation Block Diagram

to the towing speed over the range of interest. Inside the body, the impeller shaft was fitted with a disk which carried twenty equally spaced magnets. The disk rotated with the impeller shaft and the magnets on the disk passed in front of a radially fixed induction coil transducer which generated a small electrical impulse for each magnet. The series of impulses were transmitted along an electrical cable within the towing cable to equipments on the towboat wherein the impulses were amplified, shaped, and fed into a standard pulse counter. The counter, a Berkley Model 7360 EPUT (events per unit time) Meter was set to indicate the impulses accumulated during a ten-second period.

By means of a calibration which was conducted in the University of Michigan towing tank the indicated impulses per ten seconds time were converted to speed in knots. This calibration factor was 108.9 counts/10 sec and the slope of the calibration curve was linear to 0.1 of a knot.

The transducers used to indicate body depth, body roll, and body pitch were housed in a watertight container inside the towed VDS model body.

The transducer which was used to indicate body depth was a Bourns Model 2521 absolute pressure gage. This gage is a diaphragm/strain gage type with a specified range of 0 to 100 psia; a sensitivity of 4 mv/v; and a combined linearity and hysteresis of only ± 0.2 percent of full scale.

The excitation, demodulation, and signal conditioning for this

transducer was provided by a Scionics Model MCS-101 amplifier/exciter. This amplifier was also enclosed in the watertight instrumentation housing. The linear output of this amplifier is 0 to 5.0 volts dc and the gain was adjusted to provide an overall sensitivity of 43.8 millivolts per foot depth of water. The overall gain and stability of the amplifier/exciter was checked by switching from the transducer to dummy resistance bridges of known imbalance and monitoring the output; two dummy bridges were used so that drift and gain of the system could be checked.

The transducers used to indicate body roll and body pitch were Edcliff Model 5-510 damped pendulum inclinometers. Each of these transducers had a nominal full-scale range of $\pm 20^\circ$ from the reference vertical. These transducers are essentially 5000-ohm resistance potentiometers and were excited by a regulated reference dc voltage to provide 150 millivolts/degree for roll and for pitch.

A similar transducer having a nominal full-scale range of $\pm 35^\circ$ from the reference vertical was used to indicate the towstaff angle at the body. This transducer was mounted on the towpoint dynamometer and the regulated reference voltage was provided from within the watertight housing. The output of this transducer was 88.3 millivolts per degree of deviation from the vertical.

The transducer used to indicate towstaff tension at the body was a custom-designed mechanical flexure which provided the connection between the towing cable and the body towpoint. This link was instrumented with strain gages to indicate the tension applied

at the body towpoint. The gages were connected to form a resistance bridge and the ensemble was waterproofed. The resulting bridge had characteristics similar to the bridge used to indicate depth (pressure), except that the sensitivity was 1.584 millivolts per volt at full-scale tension of 350 pounds.

The excitation, demodulation, and signal conditioning for the tension strain gage bridge was also provided by a Scionics Model MCS-101 amplifier which was contained in the watertight instrument housing. The gain of the amplifier was adjusted to provide 10.25 mv per pound tension at the output. Two dummy bridges were also provided to check the drift and stability of the amplifier as in the case of the depth gage.

Except for the speed measuring device, all of the above-described instrumentation was powered from a battery package within the towed model body. The batteries were rechargeable nickel cadmium cells located in a separate watertight housing, they provided a nominal 26 volts dc. The battery package was directly connected to the instrument housing and the control (on-off) was maintained through a relay which in turn was operated from the towboat.

The instrumentation within the towed body was electrically connected to the towboat by means of six (6) individual conductors plus a shield (ground) provided by the double armor. One conductor was required to provide control and command to the instrument package; that is, commands to (1) turn "on", (2) turn "off", (3) insert dummy bridge #1 in depth and tension circuit, "Calibration #1", (4) insert

dummy bridge #2 in depth and tension circuit "Calibration #2",
(5) monitor regulated reference voltage on normal "pitch" line.
The above commands were indicated by the level of the dc voltage applied to the calibrate/command line. Circuitry within the instrumentation package provided amplitude discrimination to decode the commands and switch relays to perform the command function.

The remaining five conductors were used to monitor the dc voltage which was indicative of body roll, body pitch, body depth, towstaff tension, and towstaff angle.

The transducer used to indicate the towing tension at the surface was a Baldwin-Lima-Hamilton Load Cell Type T3P1 rated at 300 pound full-scale tension. The excitation, demodulation, and signal conditioning for this transducer was provided by a Sanborn Model 150-1100 Carrier Type Preamplifier.

The transducer used to indicate the surface towing angle was an Edcliff Model 5-510 Damped Pendulum Inclinometer similar to the one used to indicate towstaff angle. This transducer was excited from a reference dc voltage derived from a battery package in the control instrumentation.

A Sanborn Model 150 graphic recorder was provided to allow permanent recording of all signal levels except for the speed. Associated with the recorder were six preamplifiers. One of these was the above-mentioned carrier preamplifier to handle the topside tension measurement; the remaining five were direct-coupled (dc)

preamplifiers, Model No. 150-1300Z, with dc suppression so that the average signal could be suppressed and the variations recorded. Since there were six remaining signals to be recorded and only five available preamplifiers and recording channels, one channel was used for depth and roll on a time-sharing basis and selected by switch position on the control panel.

Except where it has been noted that battery power was used, all of the instrumentation was powered by 115 volts ac, single-phase, 60-cps power supplied by an ONAN gasoline-motor-driven field generator. The output voltage and frequency of this generator were meter-monitored on the instrument control panel.

Pre-test Calibration

The calibration curves for the pitch, roll, towstaff angle, and tow cable angle pendulum potentiometers were obtained using a rotary tilt table, having a graduated vernier adjustment to 0.1 of a degree.

The pressure transducer used for the depth measurements was calibrated dockside in volts per foot of depth.

The bottom tension dynamometer was calibrated in volts per pound by using known weights, meeting N. B. S. specifications, hung directly to the dynamometer.

The top tension dynamometer was checked in the same manner to assure that the calibration curve furnished with the cell was correct.

The 300-lb top tension dynamometer, as shown in Figure 9, had to be calibrated through a system, which was made up of

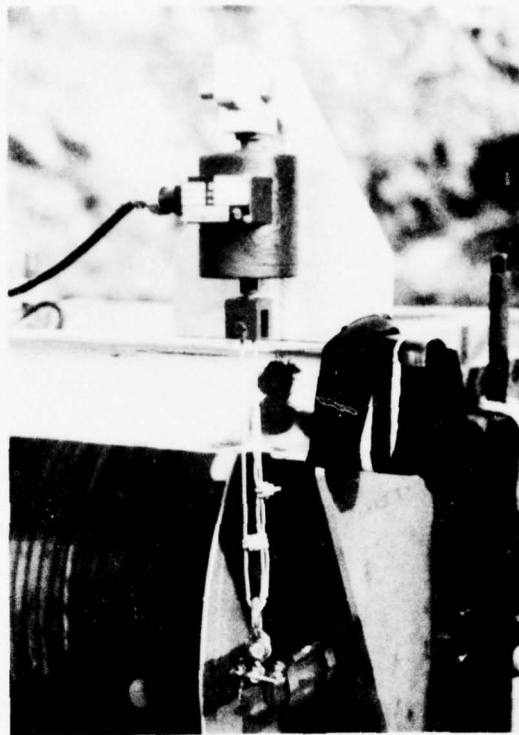


Figure 9 - Top Tension Dynamometer

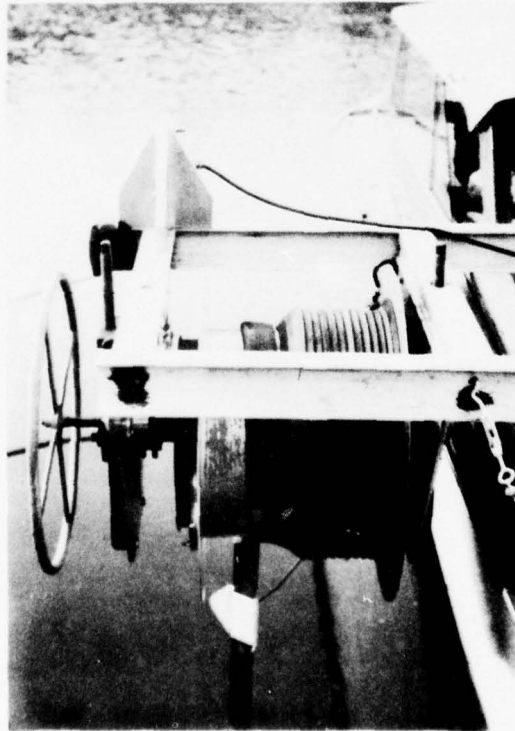


Figure 10 - Faired Cable in Test Configuration on Drum

the storage and handling drum, the 2:1 advantage arm from the drum shaft to the load cell, and the faired cable as placed on the drum.

The top tension system was set up on shore, and with the faired tow cable wrapped on the drum, known weights were placed on the cable and the calibration factor was established which converted the voltage output of the dynamometer directly to pounds of tension in the tow cable.

The lateral position of the cable on the drum had a negligible effect on the accuracy of the reading, but the attitude at which the cable made contact on the drum, other than flat, did affect the accuracy of the reading. Thus, regardless of lateral position, the fairing had to always contact the drum in a flat position. Figure 10 shows the faired cable in the correct towing position on the drum. Attention is called to how the last wrap, before entering the water, is laid flat on the drum.

With the pitch and roll potentiometers mounted in their correct position in the body, it was necessary then to establish a zero reference for each potentiometer in relation to the body. The zero reference was then established by leveling the body in the horizontal plane.

A zero reference for the towstaff angle potentiometer was established by suspending the body in a static vertical position from its tow cable beneath the drum.

A zero reference from the top tow angle potentiometer could be established only after its installation on the fairing as each scope was tested. This zero reference was valid only for that day's test.

Test Facility

The tests were conducted at the Hydrospace Research Corporation towing facility at Martinsburg, West Virginia.

The towing basin is an old stone quarry filled with water. The quarry is approximately 1,500 feet long, varies in width from 100 feet to 300 feet, and has a depth of 100 feet in the center channel.

The tow boat is a 26-foot cabin cruiser with a 10-foot beam and is powered by twin 210-horsepower marine engines. The boat housed the VDS instrument control panel, 6-channel Sanborn recorder, Hughes digital voltmeter, Beckman universal Eput Meter, and 5 K. W. 115 volt 60 cycle generator.

The custom designed towing frame was mounted just aft of midship with the drum extended over the port side of the boat as shown in Figure 5.

TEST PROCEDURE

The faired cable was wrapped on the drum as shown in Figure 10, and the body placed in the water. The body was initially towed to determine the amount of trim and ballast necessary to make it perform properly in this system.

With the trim of the body completed, the faired cable was then set at various scopes and towed over the full range of speed for each scope to assure no kiting of the system.

During the pre-data taking trials it was found that the body could be left in the water at all times with no ill effects in the system.

This eliminated the difficult handling job that was required to remove the body from the water each night. The body was only removed from the water, after this, in order to change the battery pack.

The system at this point was considered ready for test.

Each morning and before each test, the following procedures were followed to assure that the instruments were functioning correctly.

At dockside, and before each test, the instrument operator checked and recorded the battery voltage, the reference voltage, the calibration voltage, and the static readings for pitch, roll, and towstaff angle with the body in water.

The instrument operator then recorded the static reading from the bottom dynamometer with the body in the water. The body weight in water was used as a known reference.

With the scope for the test set, the operator then recorded the reading of the depth gage. This reading was checked against the known scope of towline payed out.

The top tension dynamometer reading was then checked and recorded on the data sheet. This reading should equal the weight of the body in water plus the weight of the faired cable from the center line of the drum to the towstaff of the body. This faired cable weight was comprised of the weight of the length in air plus the weight of the length in water.

The top tow angle potentiometer was then clamped to the fairing at the proper location between the drum and water. With the towline hanging vertically, the zero reference was recorded. This zero reading was used

until the clamp was moved.

The speed measuring device was then shackled to the starboard side of the towing frame and placed in the water. The electrical input lead from the speed measuring device was connected to the Beckman EPUT Meter.

The first run was made at approximately 4 knots (700 engine RPM). During the run the instrument operator adjusted the zero suppression in each channel in order to bring the electrical system back to null. At the end of the run the suppression readings and attenuator settings were recorded on the data sheet, along with the averaged towboat speed reading from the EPUT Meter. An immediate conversion of this data was made before the next run. At this time the instrument operator checked all the electrical calibrations. This procedure was repeated for every run until the entire speed range for the particular scope was completed. The immediate conversion of the data after each run was done to insure the consistency of the data taken.

The range of speeds for the test were determined by minimum and maximum RPM of the boat's engines under its operating conditions. The test runs were made from the minimum of approximately 4 knots (700 RPM), to the maximum of approximately 19 knots (3,000 RPM).

The above procedures were used on every speed run of each scope length investigated. Scope settings were made in ten-foot increments from ten feet to seventy feet.

After the tests were completed, calibrations were performed on the entire system.

TEST RESULTS AND DISCUSSIONDATA

The data are presented in Appendix A, in the form of plots of towstaff and cable, angle tension at the housing, the difference in tension at the surface and tension at the housing, and depth, each versus speed. Tare corrections have been applied to the depth and tension plots. No tare corrections were required for the angle data.

Tare corrections for the tension data arise from the weight of the top-angle measurement device, the weight of the non-wetted cable between the surface and dynamometer-drum, and the towstaff. Depth-tare arises from the location of the pressure transducer in the housing.

DATA PROCESSING

The data were converted to plots of angle versus scope for even increments of velocity from 6 to 18 knots.

A correction was applied to the towstaff angle data to adjust the values to account for the effect of a 9-inch length of bare cable between the top of the housing and the bottom of the fairing. This gap occurred as a result of various adjustments to fairing length made during the early phases of the test program to eliminate a serious tendency of the system to kite. A value for C_R of 1.4, the sine-squared loading function, measured values of T_0 were used for this correction. No correction was applied to the tension as the variation due to this cause was less than the estimated error in the tension measurement.

CONFIDENTIAL

Values of $d\varphi/ds$ and dT/ds were read from the "scope-plots" and values of F and G computed from Equations (1.1) and (2.1). The curves of angle versus scope were extended to an angle of $\pi/2$ by extrapolation of the curves backward from φ_0 . Values of $F(\pi/2)$, i. e., R , and C_R were then computed from the estimated values of $d\varphi/ds$ and $T(\pi/2)$. Finally, values of F/R , C_F , G/R , and G/V^2 were computed and plotted against angle.

RESULTS

The variation of the normal force coefficient, C_F , with angle of inclination is shown on Figure 11. The normal force coefficient, C_F , is defined as $F/(1/2 \rho V^2 d)$, where d is the maximum thickness of the fairing. The variation of F/R with angle is shown on Figure 12.

The variation of tangential force, reduced on the same basis as F and plotted as G/R is shown on Figure 13.

The values of R and C_R are shown on Figure 14.

DISCUSSION

The values of C_R deduced from these data exceed two-dimensional values measured in the wind-tunnel and water channel by a factor of from 1 to 1.25. These values are subject to the criticism that they were obtained by extrapolation of the cable angle data. They must, however, exceed the values of F deduced from the curvatures at φ_0 and as these values are generally greater than the previously referenced values of C_R , there can be no doubt that the in-situ resistance as measured is greater than indicated by the

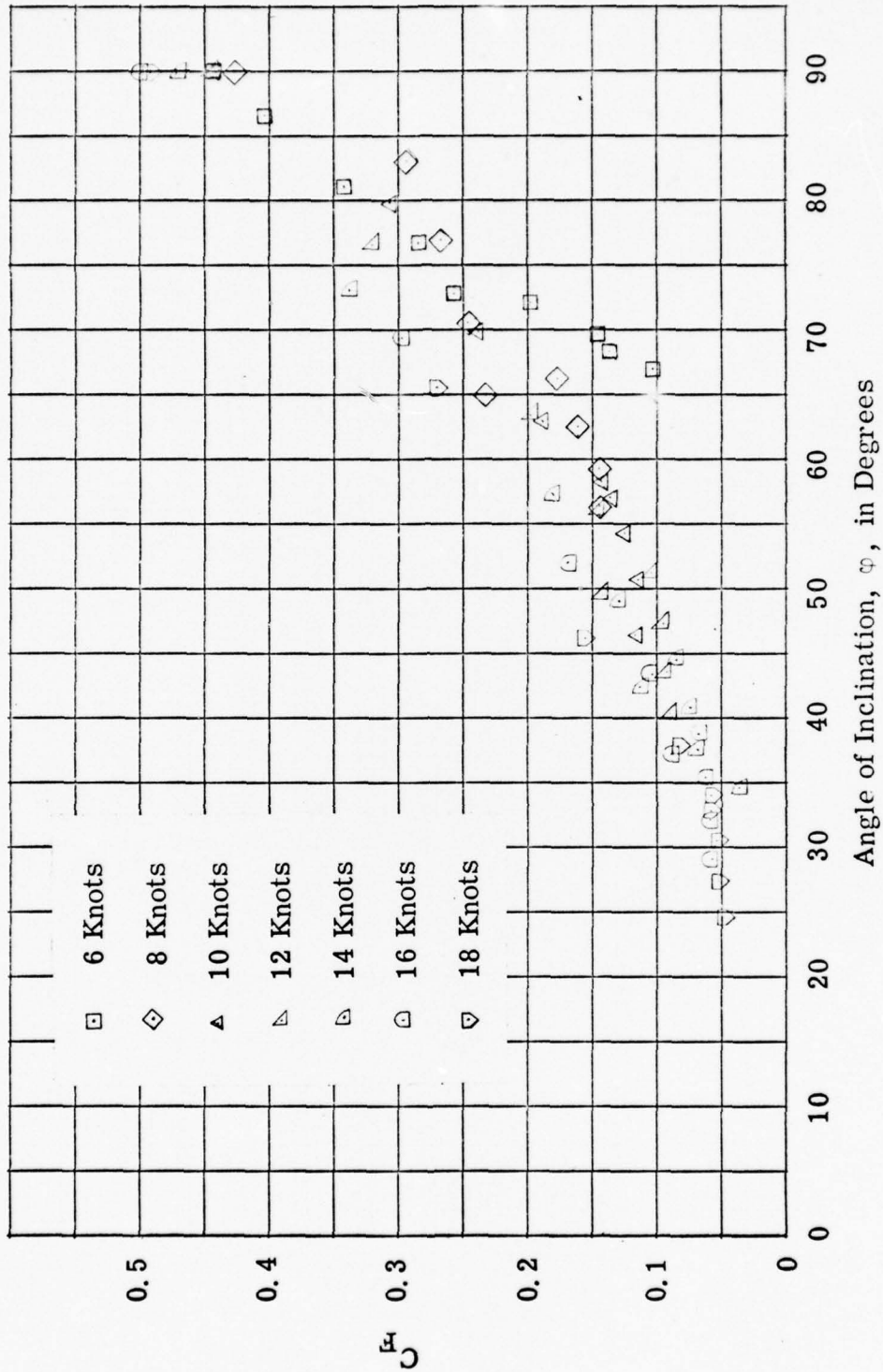


Figure 11 - Normal Force Coefficient vs Angle of Inclination

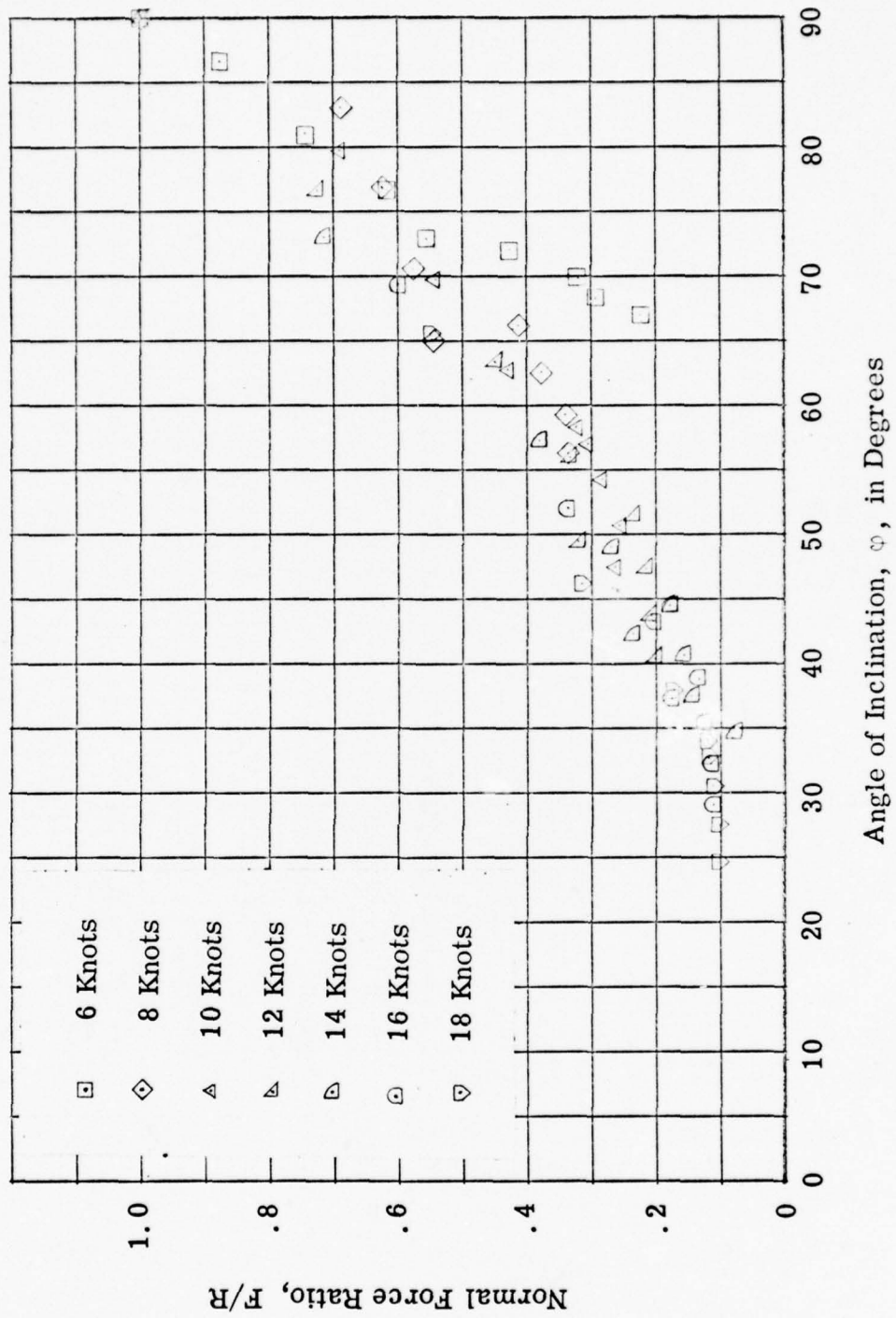


Figure 12 - Normal Force Ratio vs Angle of Inclination

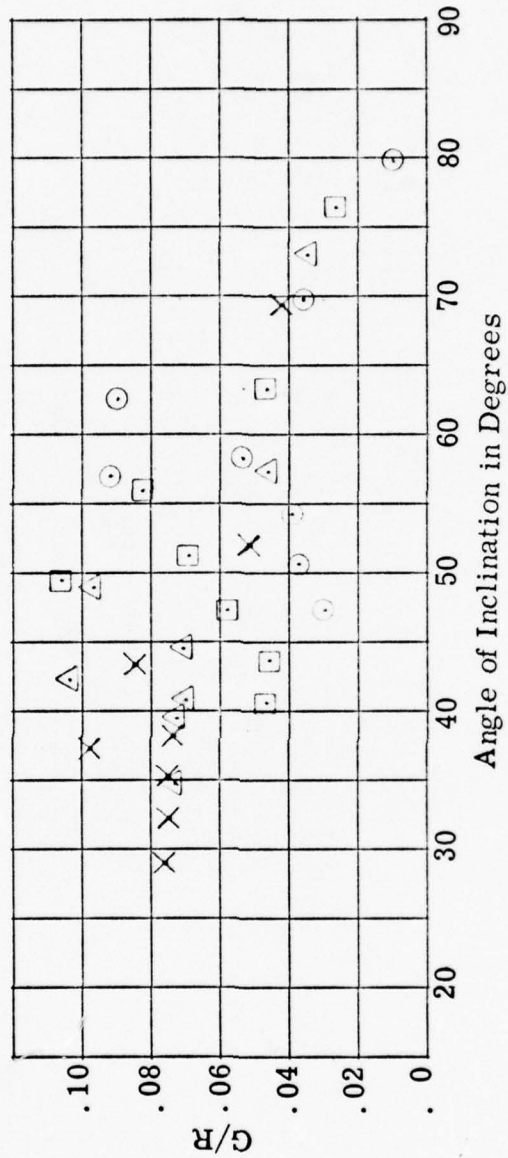


Figure 13 - Tangential Force Ratio vs Angle of Inclination

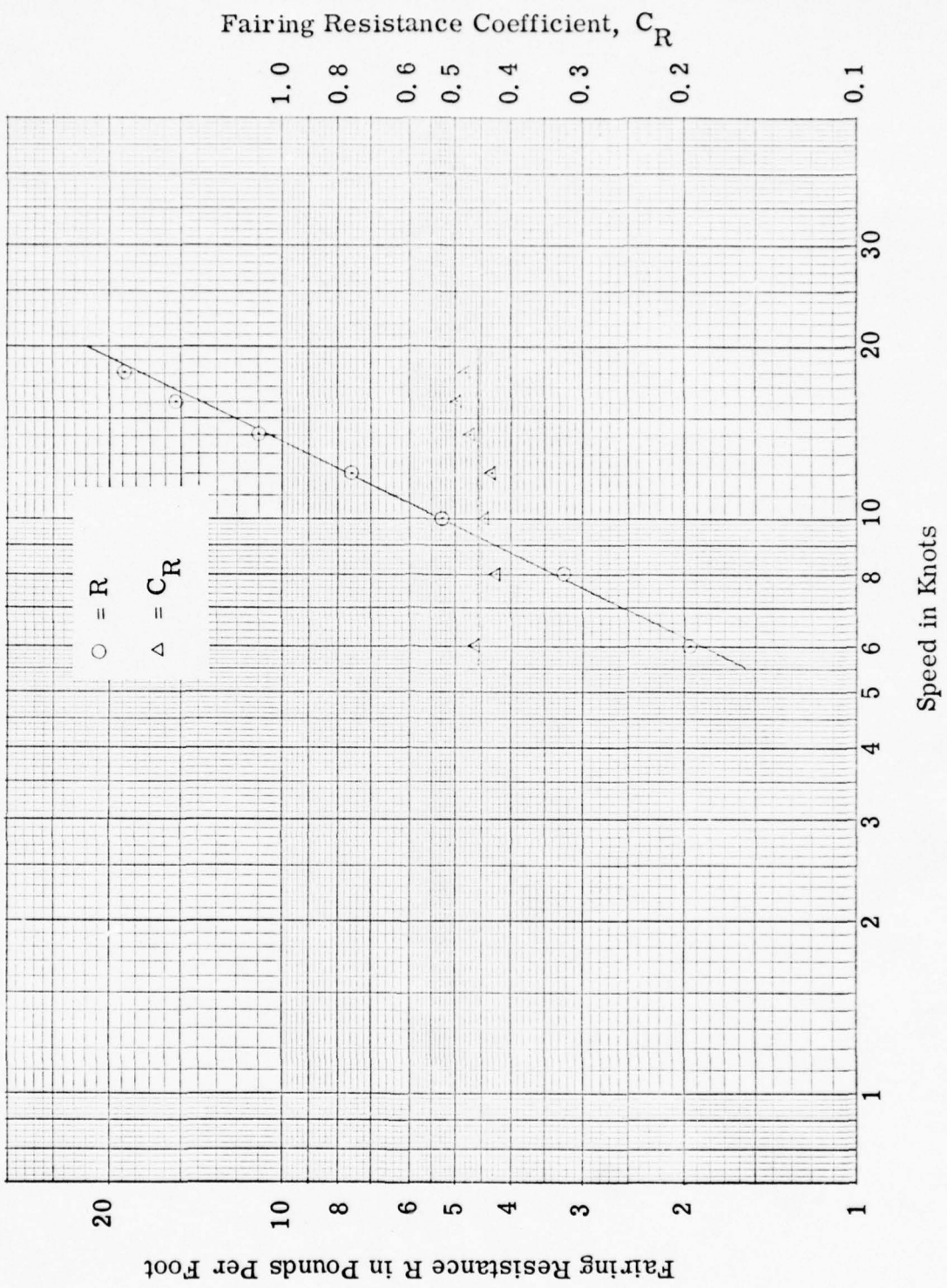


Figure 14 - Fairing Resistance and Resistance Coefficient vs Speed

previously determined two-dimensional values.

The values of F/R group about a curve that falls well under the classic "sine-squared" result and, of course, well below the $a \sin^2 \varphi + b \sin \varphi$ representation. There is no doubt concerning the validity of these data insofar as they represent the physical situation pertaining to this test.

Two questions must be resolved prior to general acceptance of these results. The first is that discussed earlier under the section entitled, "Test Theory and Design". Namely, is the measure of angle and tension at all points along the cable independent of the existence of the towline that lies above the point? This question has not been answered. The second concerns the effect of the surface. An aeration cavity and some wave-making occurs. The resistance due to wave-making is probably not negligible as constant (atmospheric) pressure prevails over the non-wetted surface and hence normal recovery of the dynamic pressure cannot occur. A higher resistance would then be expected than in fully wetted flow.

The effect of a higher resistance acting over an appreciable length of the first ten feet of the fairing would be to introduce a sharp curvature in that section. The effect on each succeeding increment of fairing would be proportionately less as the angle of water entry is successively less steep. The curvatures measured at the surface would then more nearly approach those that would exist in the absence of cavitation. The net result then would be a downward tilting of the F/R curve.

Therefore we must inquire as to the extent or degree to which a possible artificially high resistance of the initial section of fairing influences the results presented herein. It was observed that only one to two feet of the fairing (10 to 20% of the immersed length) were affected by the aeration cavity at speeds below about 10 knots. The affected length gradually increased with speed, reaching a value of four to five feet at the highest speeds run. It would thus be expected that the resistance at the lower speeds would be proportionately less than those observed at the higher speeds. A slight increase in C_R was observed at the higher speeds. The increase is small, however, and believed insufficient to indicate significant aeration effect on the resistance. Nevertheless, until conclusively demonstrated to the contrary, it cannot be presumed that the aeration cavity introduced a second order effect.

An anomaly was observed in the variation of angle with scope. This may be seen on Figure A-2* as a reversal in order of the 30- and 40-foot scopes. It is more strikingly demonstrated on the plots of angle against scope, Figures 15 and 16, as a discontinuity in the curves. The discontinuity cannot be ascribed to instrument error as the 30-foot scope data is the composite of 2 tests interspersed among the tests of other scopes and the 40-foot scope data is the composite result of 3 tests similarly spread in time. No ready explanation is available. It is conjectured that the effect results from a change in boundary layer characteristics for which the 40-foot

*See Appendix A.

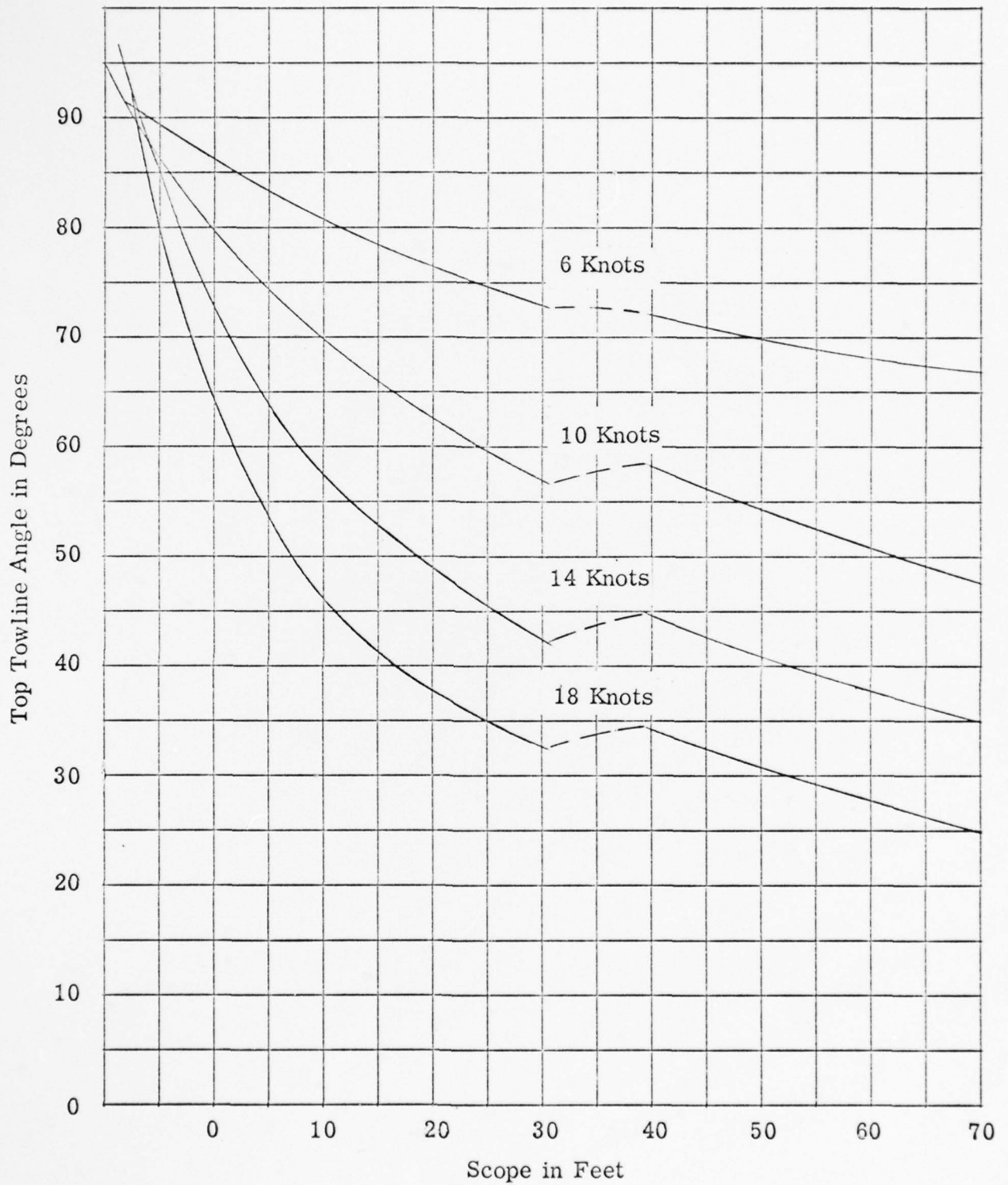


Figure 15 - Top Towline Angle vs Scope in Feet

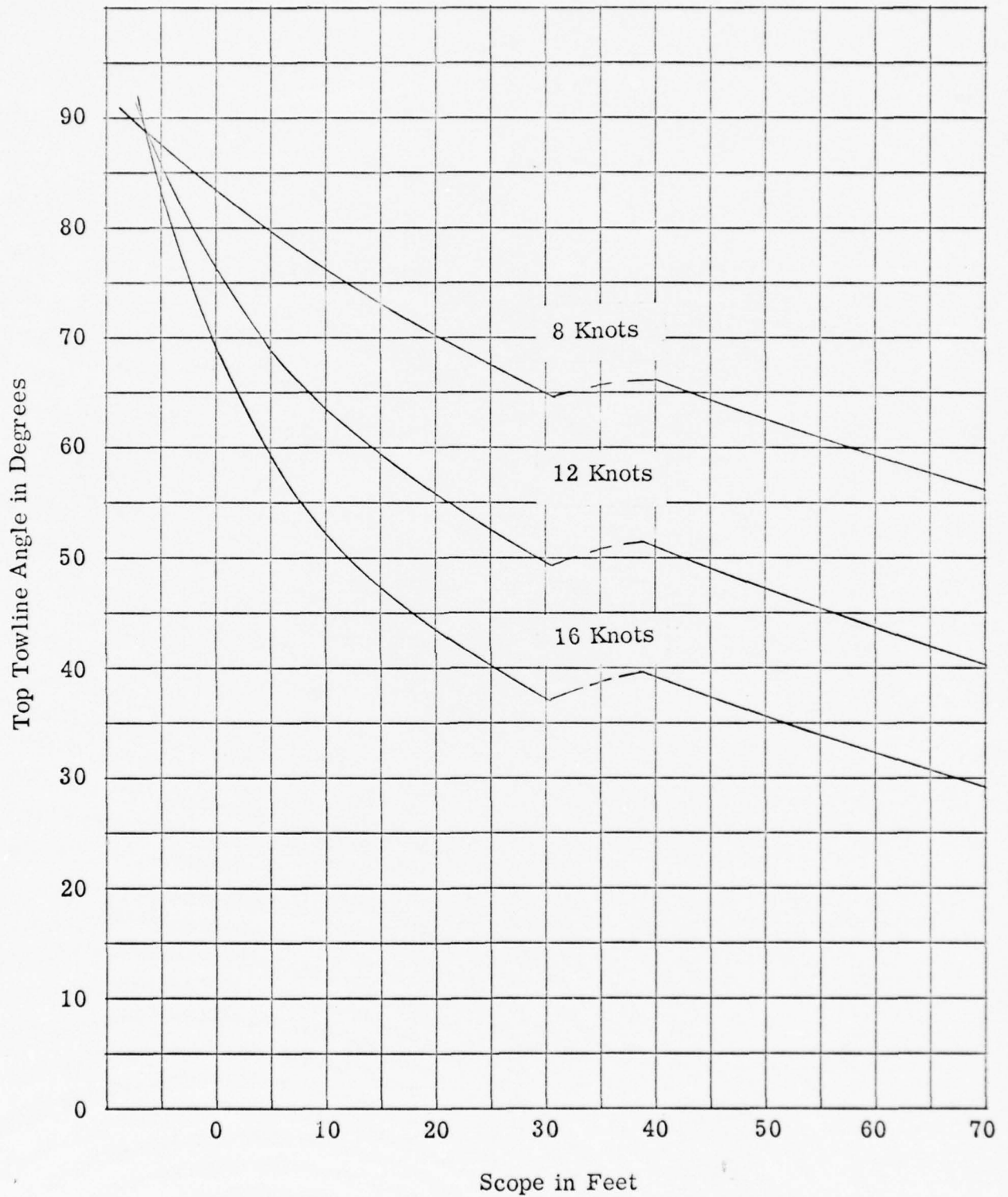


Figure 16 - Top Towline Angle vs Scope in Feet

scope represents a critical length. It may possibly be associated with the aeration phenomenon. It remains to be resolved.

The curves of the increment of tension against scope show an initial steepening as the angle shallows (Figure 17) followed by an apparently slight decrease in the rate of increase with scope thereafter. The plots of F/R (Figure 12) are similar to those resulting from Powell's data (Figure 1) and the AEW data.

The scatter in these data preclude judgement concerning the existence of a maximum as indicated by the two-dimensional data referenced above.

The scatter in these data is believed to result from three causes: the sensitivity of tension to changes in housing pitch due to the fact that a large percentage of tension was produced by hydrodynamic lift, the unsteady forces introduced by the aeration cavity, and the accuracy with which the final tension determinations could be made. The mean pitch-angle of the housing varied by no more than $\pm 3/4$ -degree from run to run at equal speeds, with starting a mean value of six degrees at four knots and gradually decreasing to a mean value of 2.5-degrees at 18 knots. Variations within the run did not exceed ± 0.8 degrees. The resulting spread of the means of the tension at the housing is shown in Figure A3 and of the towstaff angle on Figure A1. The basic sensitivity of the dynamometer used for the measure of cable tension at the surface was ± 0.6 lb., or 0.1% of full scale. The attenuation required to decrease the amplitude of the signal fluctuations, however, reduced the

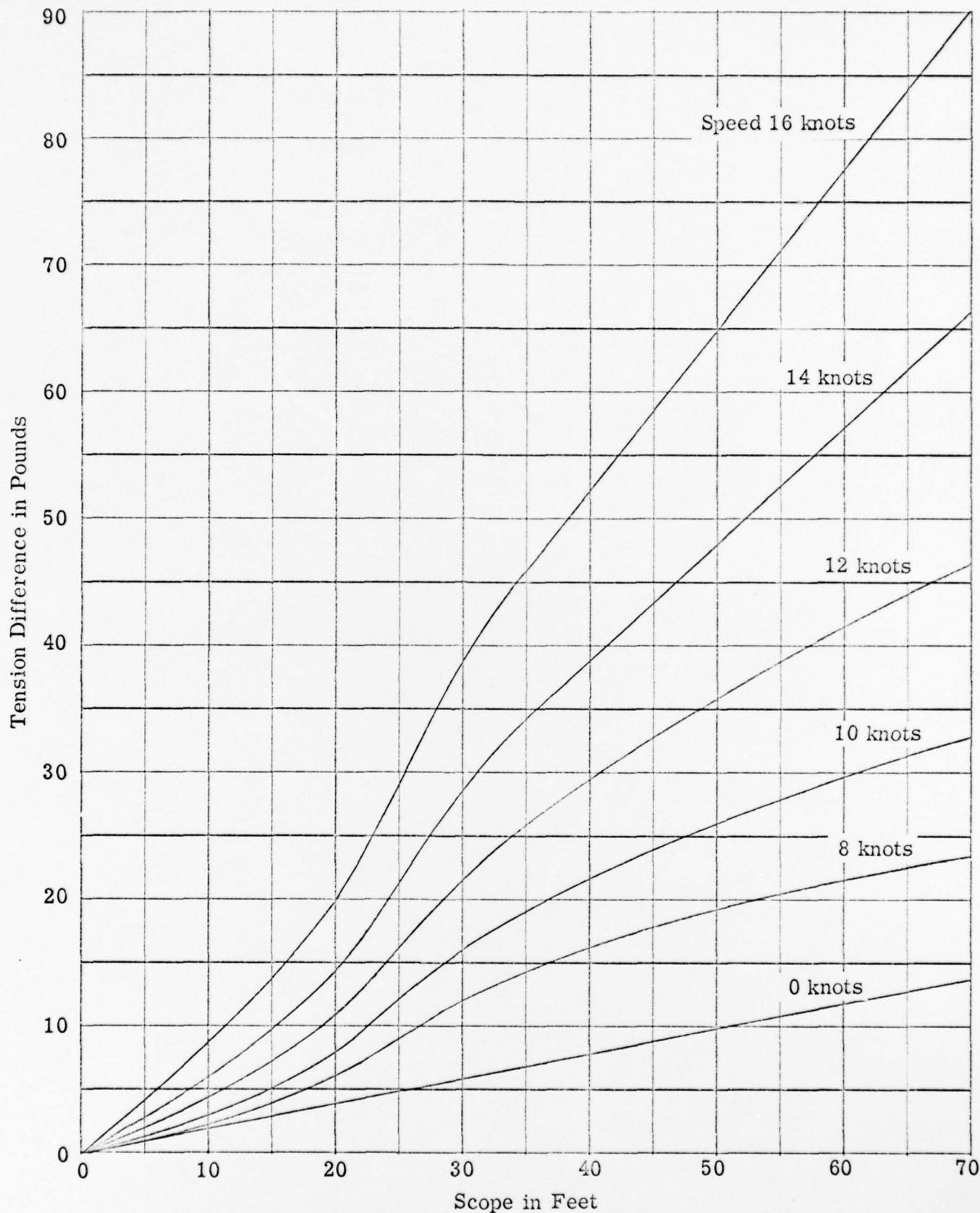


Figure 17 - Top - Bottom Tension Difference vs Scope

available sensitivity such that a one-millimeter deflection of the pen on the chart paper corresponded to 6 pounds of load. It was observed that the operator could not reliably establish the null position to within 1 mm. The cable-tension and top angle channel required the greatest attenuation, and hence exhibited the maximum fluctuation of mean value. It is believed that elimination of the aeration effect and the use of a housing less hydrodynamically sensitive to pitch effects will significantly decrease the scatter in the top tension channel. It should also lead to improvements in the other channels of information.

To conclude this discussion, some remarks are in order concerning the remedies utilized to eliminate the tendency of the fairing to kite. Tests were commenced with a 50-pound body weight, the objective being to run with three different weights so as to produce cable configurations of different initial curvatures. The fairing was found impossible to stabilize at body weights of 50 and 100 pounds and was stabilized at the 150 pound (test) weight only after taking great care in the assembly to avoid any initial tension in the fairing itself. It is believed that this represents a marginal condition, however, for this particular piece of fairing, inasmuch as it would on occasion kite severely on first immersion following overnight storage on the drum, or first immersion on a cold morning after overnight exposure.

CONCLUSIONS AND RECOMMENDATIONS

The results of the tests described herein give indication that strong three-dimensional effects prevail in a real faired-cable configuration, with the reservation that the results are influenced to an unknown extent by surface effects. The results indicate that it is feasible to obtain in-situ measures of fairing characteristics under suitably controlled conditions.

The results must be considered tentative until such time as the degree of the surface effect is established and (more mildly) until such time as comparison can be made between the two experimental procedures discussed under "Test Theory and Design".

The following recommendations are presented for consideration:

- 1) Have the elastic characteristics of the fairing-piece-tested determined by the manufacturer and compared with the "as-molded" specifications.
- 2) Conduct further tests to establish the degree of the surface effect and to determine the extent to which elimination of the aeration cavity decreases system-force fluctuations.
- 3) Utilize a non-winged body of revolution for future tests to
 - a) decrease body-generated force fluctuations and
 - b) work at higher values of the starting angle.
- 4) On resolution of the surface-effect question, characterize the fairing for several body weights, i. e., for several values of the initial curvature at a given speed.
- 5) Characterize at least two other fairings representative of a class (trailing and sectional for example) and one bare, smooth cable.

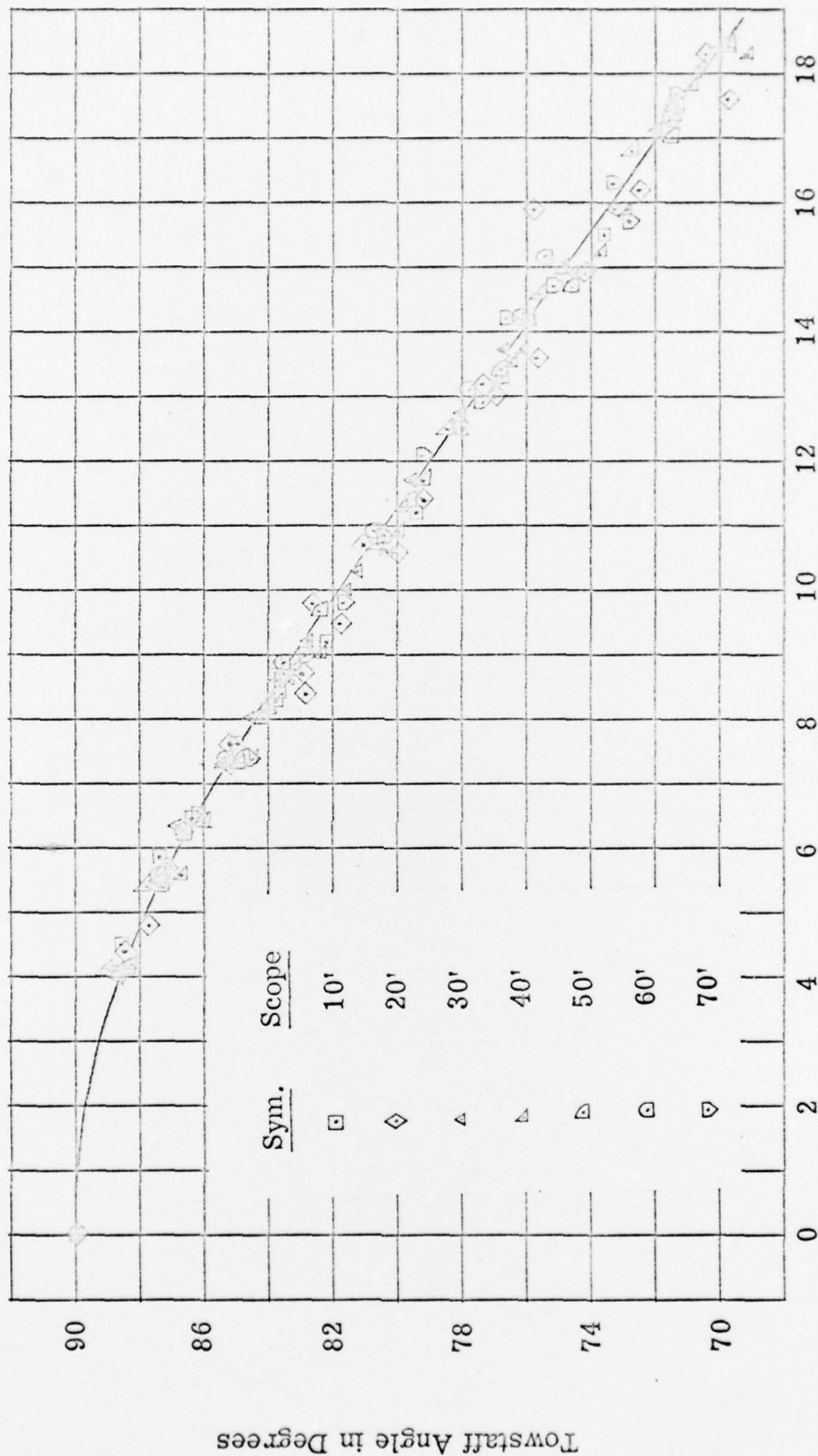
REFERENCES

1. Pode, Leonard, "Tables for Computing the Equilibrium Configuration of a Flexible Cable in a Uniform Stream," David Taylor Model Basin Report No. 687, March, 1951.
2. Relf, E. F. and C. H. Powell, "Tests on Smooth and Stranded Wires Inclined to the Wind Direction, and a Comparison of Results on Stranded Wires in Air and Water," R and M 307, January, 1917.
3. Glauert, H., "Heavy Flexible Cable for Towing a Heavy Body Below an Aeroplane," R. and M 1952, February, 1934.
4. Reber, R. K., "The Configuration and Towing Tension of Towed Sweep Cables Supported by Floats," Report No. 75, Mine-Sweeping Section, Bureau of Ships, Department of the Navy, Washington, D. C., February 18, 1944.
5. Eames, M. C., "The Configuration of a Cable Towing a Heavy Submerged Body from a Surface Vessel," Naval Research Establishment (Canada), Report No. PHx-103, November, 1956.
6. Whicker, L. F., "The Oscillatory Motion of Cable-towed Bodies," University of California Report Series No. 82, Issue No. 2, 1957.
7. Powell, C. H., "The Resistance of Inclined Struts," R and M 599, March, 1919.
8. Lofft, R. F., "Variable Depth Asdic Resistance and Lift of Cable Fairing when Inclined to Direction of Flow," Admiralty Experiment Works, Report No. 31/58, July 1958. (SECRET)

CONFIDENTIAL

APPENDIX A

CONFIDENTIAL



Speed in Knots
Figure A1 - Towstaff Angle vs Speed

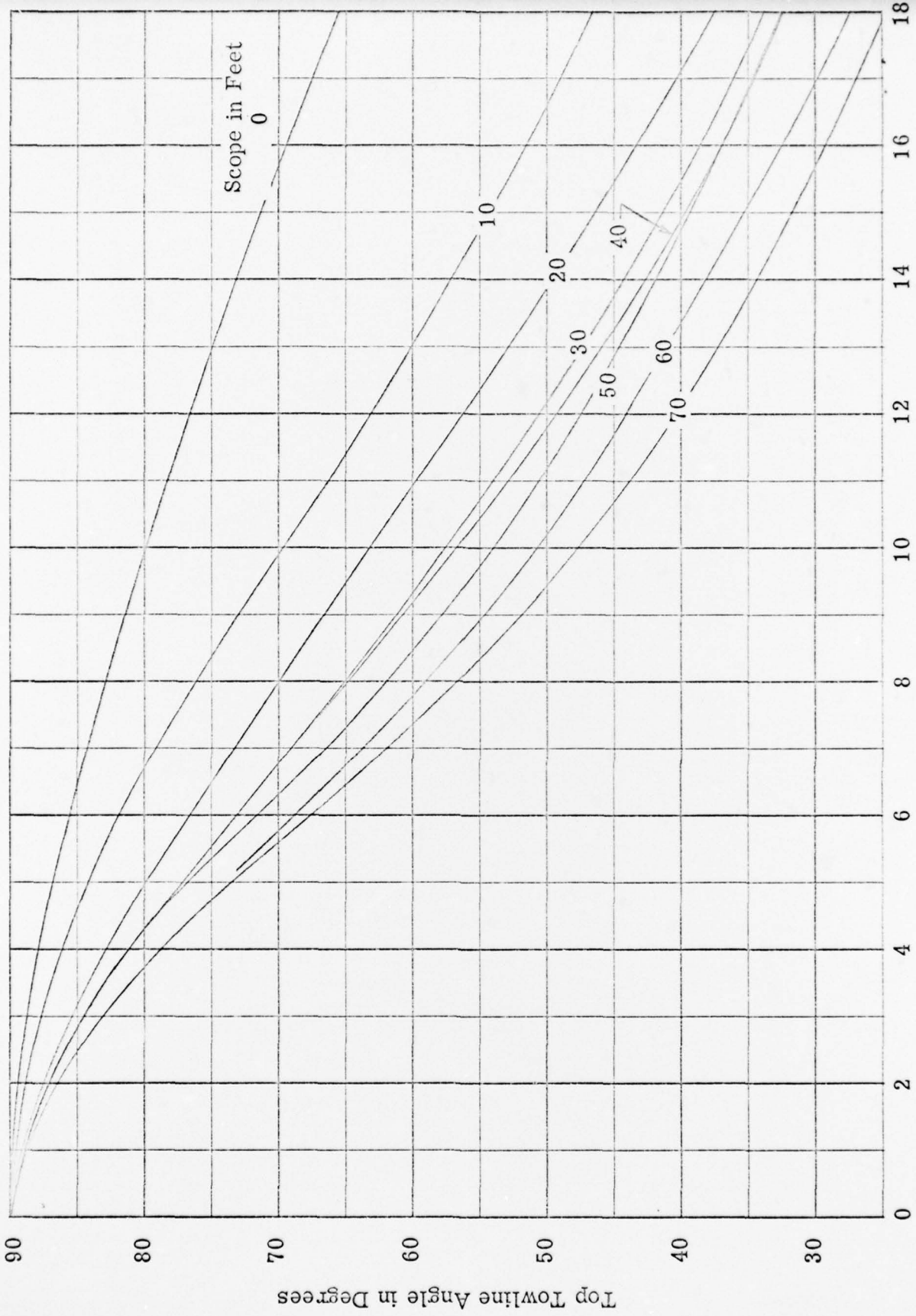


Figure A2 - Top Towline Angle vs Speed

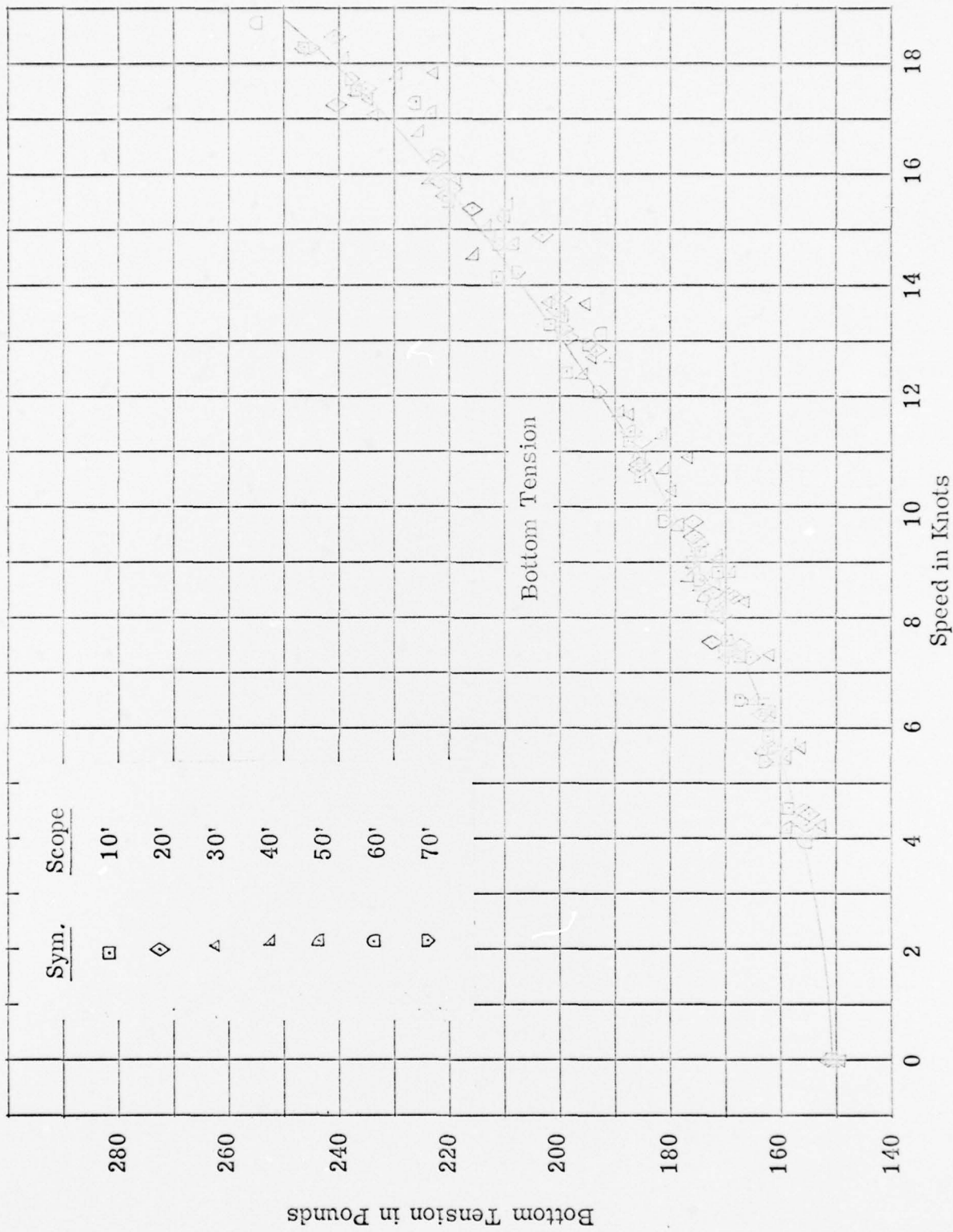


Figure A3- Bottom Tension vs Speed

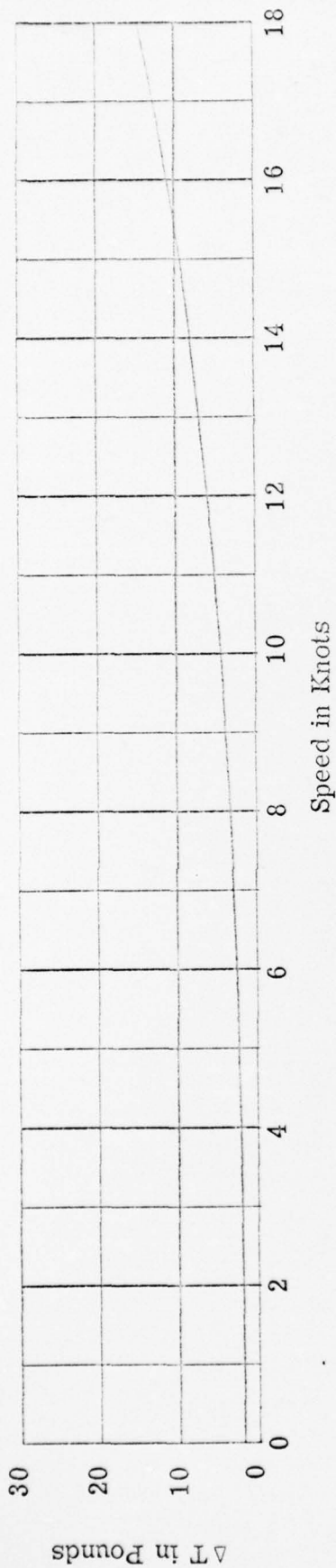


Figure A4.- Top-Bottom Tension Difference - 10 ft. Scope

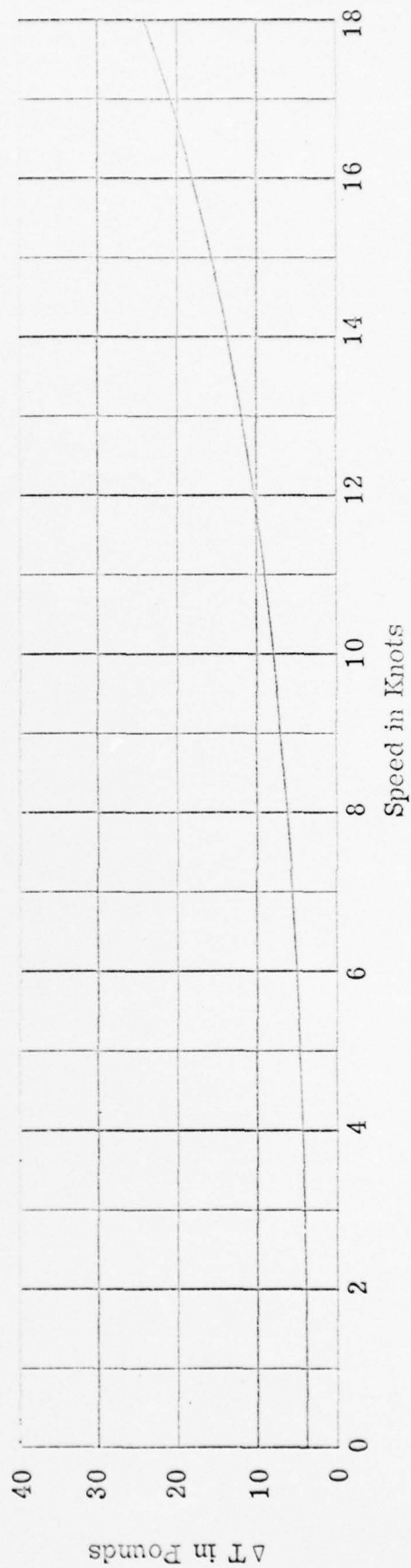


Figure A5.- Top-Bottom Tension Difference - 20 ft. Scope

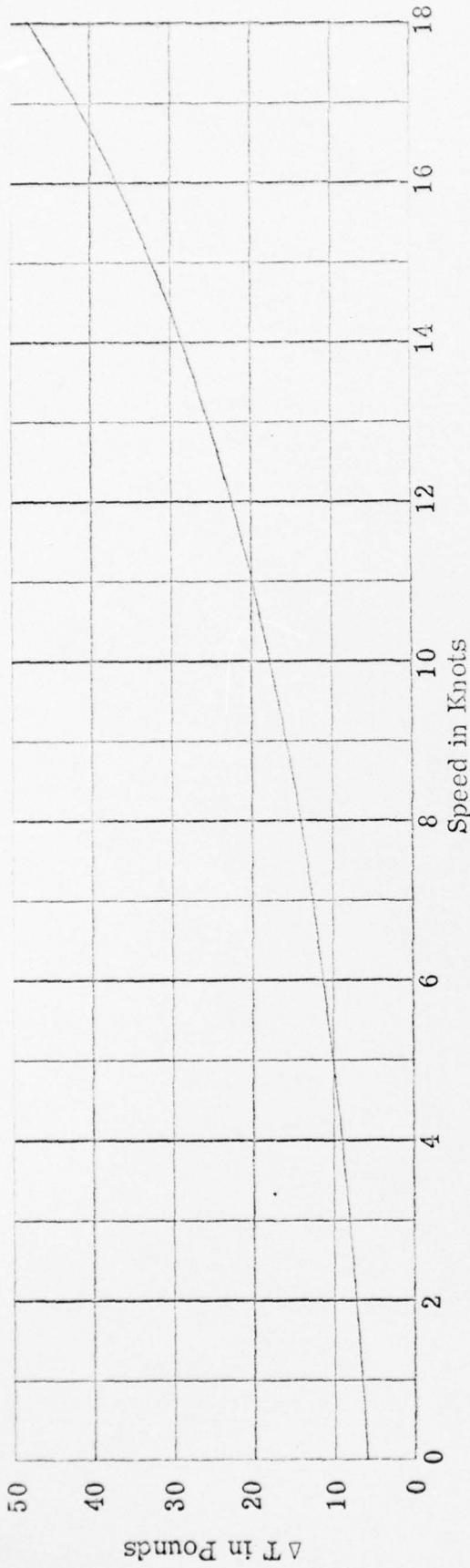


Figure A6 - Top - Bottom Tension Difference - 30 ft. Scope

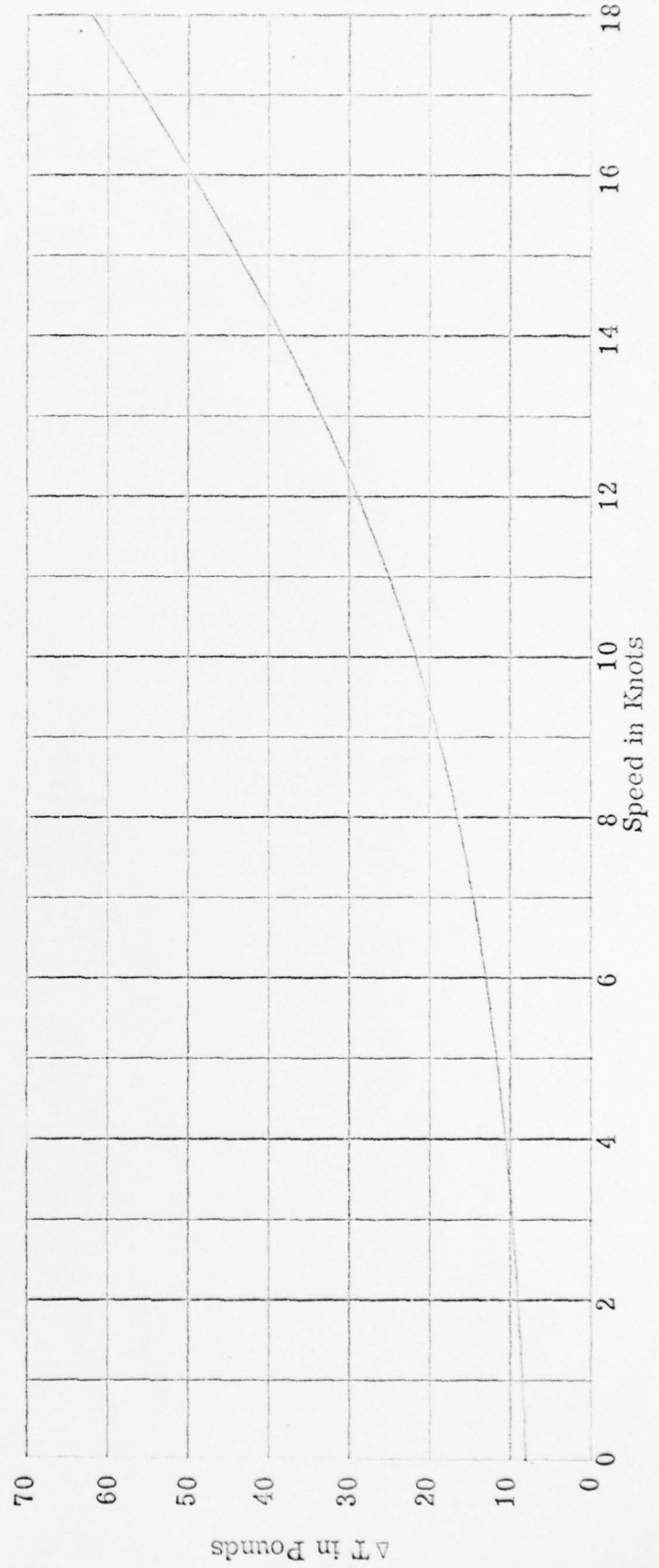


Figure A7 - Top - Bottom Tension Difference - 40 ft. Scope

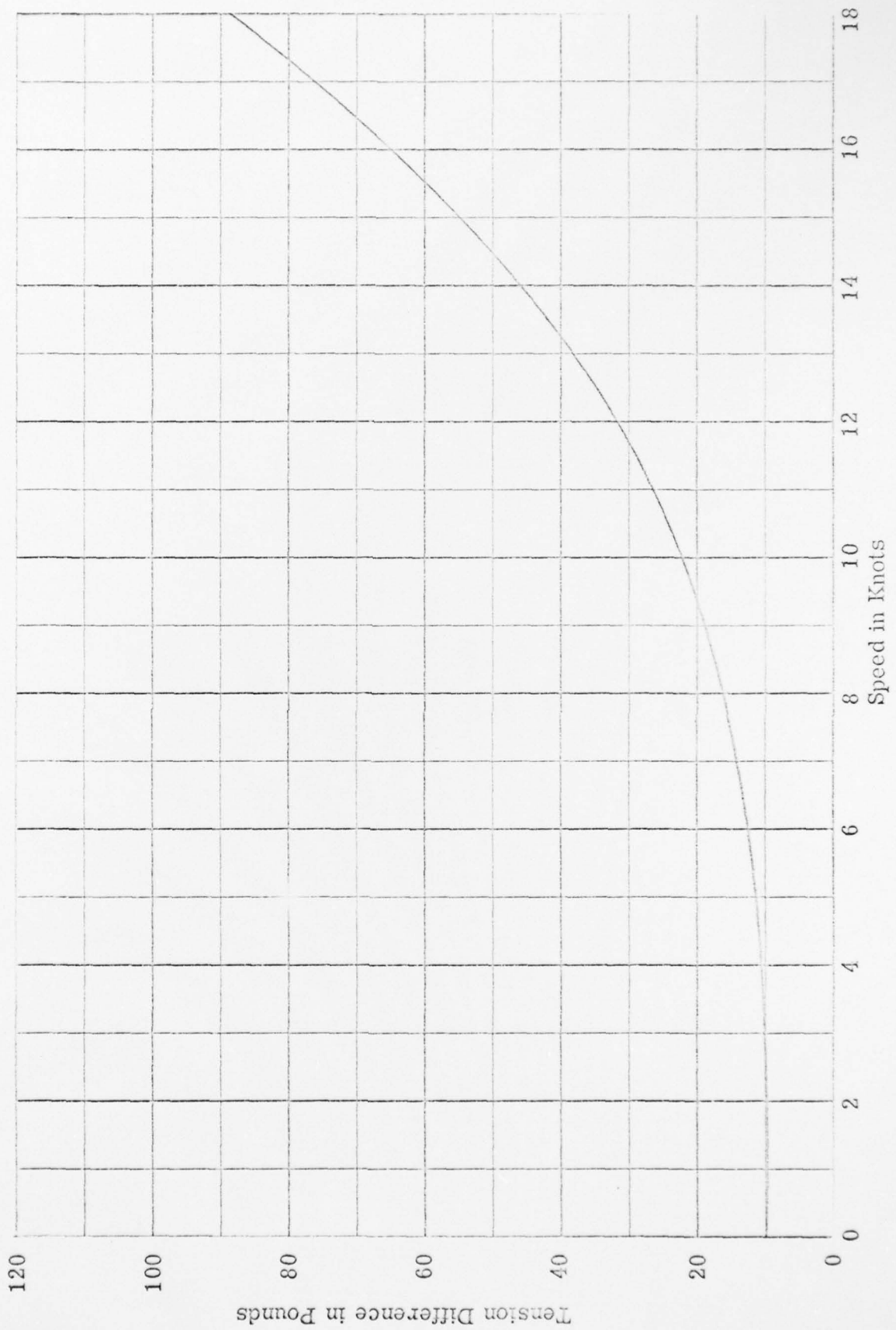


Figure A8.- Top-Bottom Tension Difference - 50 ft. Scope

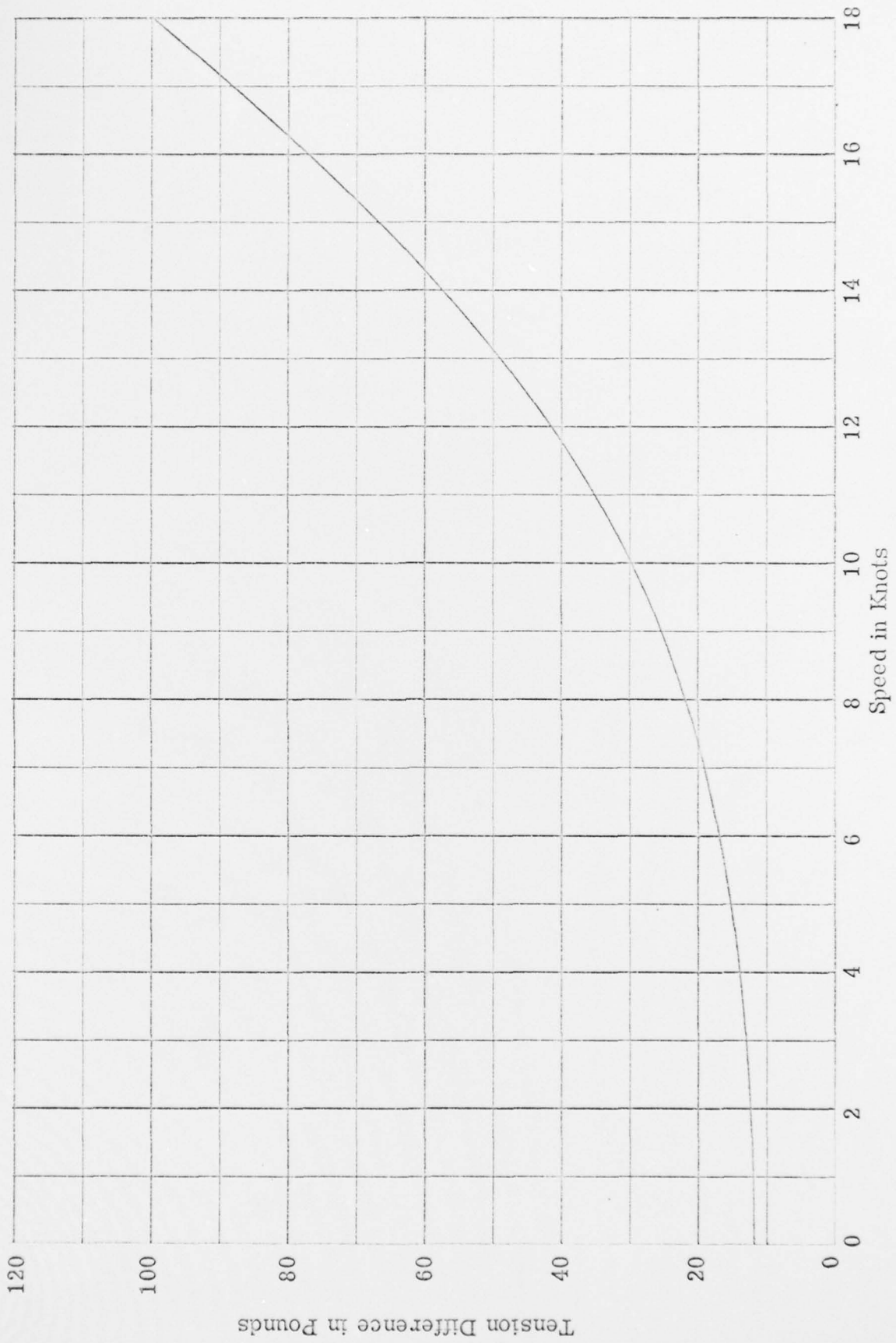


Figure A9 - Top-Bottom Tension Difference - 60 ft. Scope

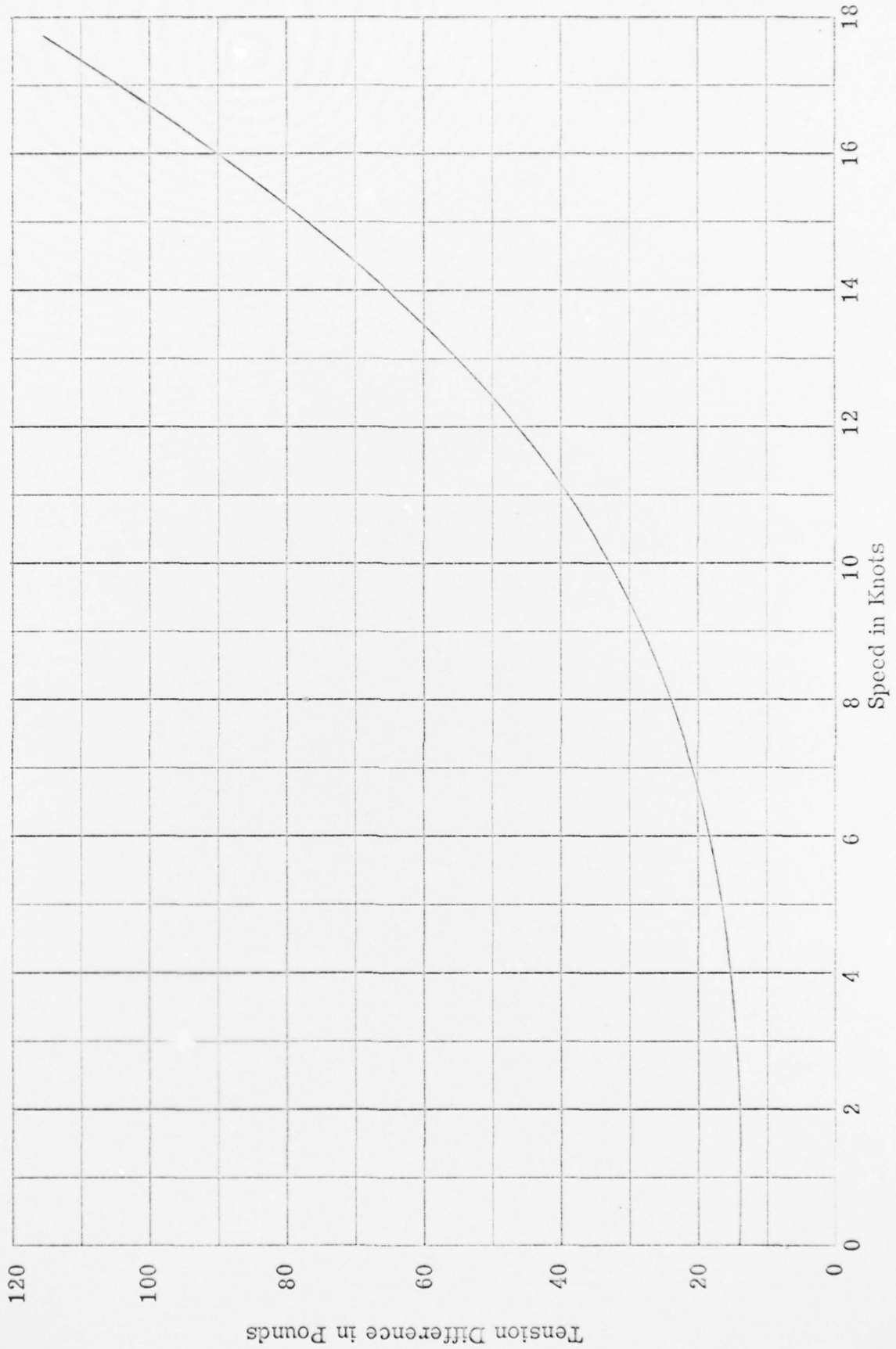


Figure A10. Top-Bottom Tension Difference - 70 ft. Scope

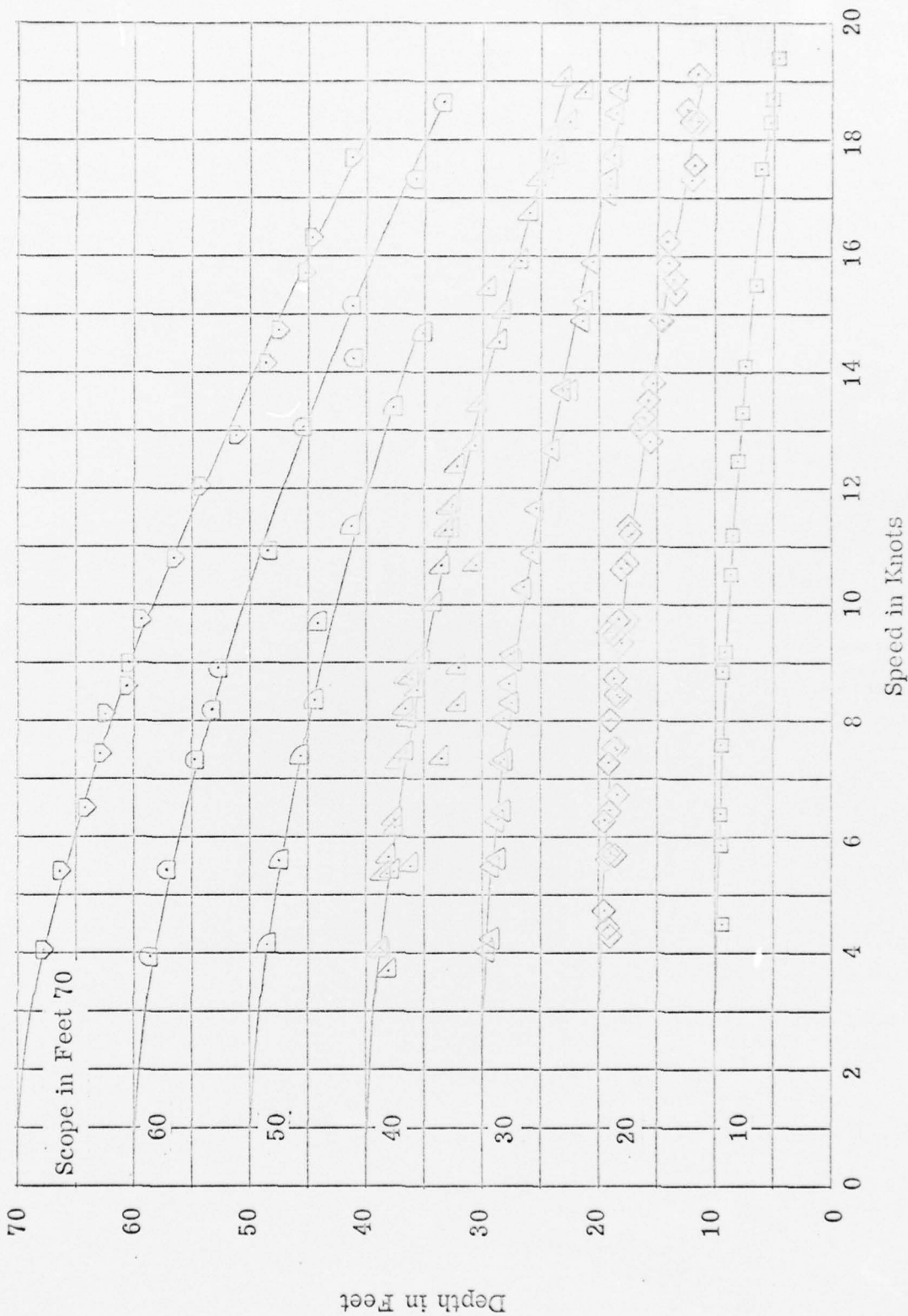


Figure A11- Depth vs Speed